AD-A036 984 ARIZONA UNIV TUCSON DEPT OF PHYSICS F/G 7/4
INTRODUCTION TO AND REVIEW OF BEAM-FOIL SPECTROSCOPY,(U)
JAN 77 S BASHKIN N00014-75-C-0499
UNCLASSIFIED NL

1 OF 1
AD A036 984

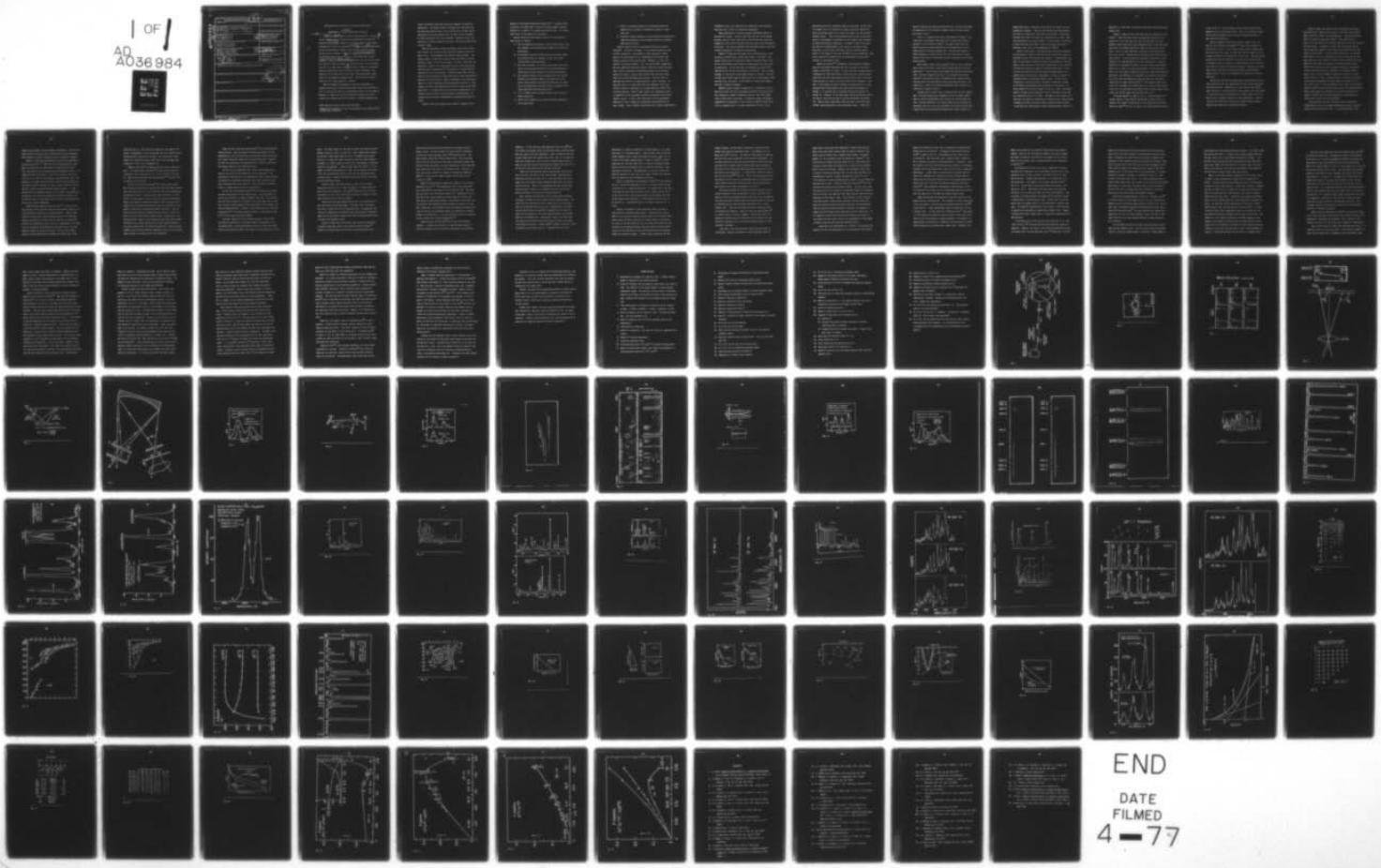

END
DATE FILMED
4-77

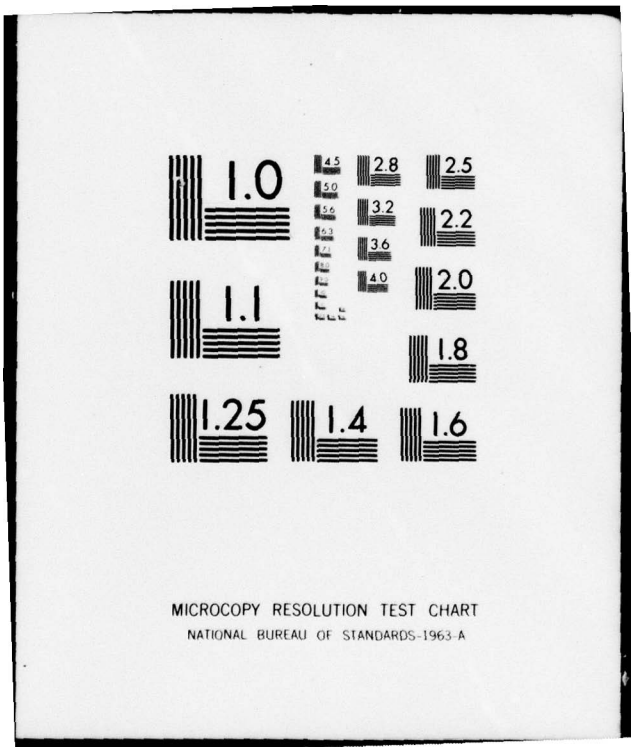
1.0
1.1
1.25
1.4
1.6
1.8
2.0
2.2
2.5
2.8
3.2
3.6
4.0
4.5
5.0
5.6
MICROCOPY RESOLUTION TEST CHART
NATIONAL BUREAU OF STANDARDS-1963-A

AD A036984

SECURITY CLASSIFICATION OF THIS PAGE (When Data Entered)

REPORT DOCUMENTATION PAGE

READ INSTRUCTIONS BEFORE COMPLETING FORM

1. REPORT NUMBER
2. GOVT ACCESSION NO.
3. RECIPIENT'S CATALOG NUMBER

4. TITLE (and Subtitle)
Introduction to and Review of Beam-Foil Spectroscopy

5. TYPE OF REPORT & PERIOD COVERED

6. PERFORMING ORG. REPORT NUMBER

7. AUTHOR(s)
Stanley Bashkin

8. CONTRACT OR GRANT NUMBER(s)
N00014-75-C-0499

9. PERFORMING ORGANIZATION NAME AND ADDRESS
University of Arizona
Tucson, Arizona 85721

10. PROGRAM ELEMENT, PROJECT, TASK AREA & WORK UNIT NUMBERS

11. CONTROLLING OFFICE NAME AND ADDRESS
Office of Naval Research
Physics Program Office
Arlington, Virginia 22217

12. REPORT DATE
January 1977

13. NUMBER OF PAGES
92

14. MONITORING AGENCY NAME & ADDRESS(if different from Controlling Office)
Same

15. SECURITY CLASS. (of this report)
Unclassified

15a. DECLASSIFICATION/DOWNGRADING SCHEDULE

16. DISTRIBUTION STATEMENT (of this Report)
Approved for public release; distribution unlimited.

17. DISTRIBUTION STATEMENT (of the abstract entered in Block 20, if different from Report)

18. SUPPLEMENTARY NOTES

19. KEY WORDS (Continue on reverse side if necessary and identify by block number)

20. ABSTRACT (Continue on reverse side if necessary and identify by block number)

DD FORM 1 JAN 73 1473 EDITION OF 1 NOV 65 IS OBSOLETE
S/N 0102-LF-014-6601

SECURITY CLASSIFICATION OF THIS PAGE (When Data Entered)

Introduction to and Review of Beam-Foil Spectroscopy*

S. Bashkin
Department of Physics, University of Arizona

This paper is the ~~I have~~ divided ~~my~~ subject into four separate parts. In the first, ~~I review~~ some of the historical developments of beam-foil spectroscopy are reviewed and ~~give~~ examples from various stages in the increasing sophistication of the experiments are given. ~~In~~ the second part ~~I~~ concentrates on the determination of spectra from different stages of ionization of various elements. ~~In~~ the third, ~~I turn my attention to~~ is concerned with the determination of the lifetimes of excited electronic states. ~~Finally, I shall say something about~~ The last part deals with problems which will occupy beam-foil groups in the near future. I should say that it will be necessary for me to omit certain important topics, especially the phenomena of quantum beats and the emission of Auger electrons. Fortunately, we will hear later in the week from Jürgen Andrä, whose paper will be devoted to quantum beats. For the latter subject, I refer you to a recent paper by I. Sellin.[1]

While the general arrangement of beam-foil experiments is probably known to you, let me refresh your memories by referring to Fig. 1. We see that there is an accelerator which, for illustrative purposes, is taken to be a Van de Graaff accelerator, but which could be any kind of positive ion machine. Isotope separators and

*Work supported in part by NSF, ONR, and NASA.

linear accelerators have been used quite commonly for beam-foil experiments. The range of particle energies over which the work has been done extends from as low as 50 keV up to 110 MeV, and an experiment has now been approved for the Super Hilac at Berkeley in which the beam will be iron at 500 MeV. Needless to say, the questions of interest change as one varies the particle energy over so wide a range.

When the beam emerges from the machine, some kind of deflector is used so as to extract that particular component which one wants to use. That component then enters a target chamber. The target chamber is some sort of can in which the target is always the same, namely, a thin film of carbon. By thin, I mean that the thickness is about 5 to 10 microg/cm^2 for most of the experiments. The beam passes through the foil and emerges in various stages of ionization as well as excitation. Excited systems decay to lower states with the emission of light; that light is then examined with some sort of optical device. What is indicated in this particular figure is a fast spectrograph with photographic recording; it represents the Meinel spectrograph which we used in many of our early experiments. In recent years we have turned to photoelectric recording, and have used a variety of types of spectrometers, including normal-incidence, Seya-Namioka, and grazing-incidence devices.

Figure 2 shows what happens when a beam of nitrogen with an

energy of 2 MeV passes through the carbon foil.[2] The beam, which is entirely invisible when it enters the target chamber, becomes luminous as a result of its interaction with the foil. It is this light which is the subject of our studies.

We may summarize the principal properties of the beam-foil light source as follows:

1. One can examine every element in the periodic table, since all elements can be accelerated in some kind of particle accelerator.
2. By changing the particle energy, one can vary the number of electrons which are removed, so that even highly-ionized atoms become accessible.
3. The light originates in a vacuum, which means that radiations in the vacuum ultraviolet can be studied merely by connecting the target chamber to a vacuum spectrometer.
4. The constant velocity of the emitters means that one can determine the temporal change in the population of an excited spectroscopic term merely by measuring the intensity of an appropriate spectral line as a function of distance downstream from the exciter foil.
5. It is a simple matter to apply external field to the radiating particles.
6. There is no residual gas to cause collisional damping of the excited terms.

7. There is a complete absence of the bremsstrahlung background which is present in traditional sources of light from ions.
8. By paying careful attention to the acceleration and particle-selection processes, one can produce emitters of unusually high chemical purity.

Figure 3 shows some early spectrograms[2] made with a Meinel instrument. The beam is nitrogen. It is traveling upward in each of these photographs. Each streak of light represents a photograph of the spectrometer slit, illuminated by the several wavelengths radiated by the particle beam. Figures a, b, and c correspond to different energies: 0.5, 1.0, and 2.0 MeV, respectively. One sees immediately that many spectral lines were excited and that their relative intensities varied significantly as the particle energy was changed. One can also see that some lines are rather long, while others disappear quite quickly. Thus one finds immediately that there is a large variation in level lifetimes. On the other hand, it is also clear that the photograph, while capturing a wealth of information in a single exposure, suffers from a serious handicap. Most of these lines are so overexposed that it is impossible to get reasonable intensity information from a densitometer tracing. In fact, some lines which are not overexposed along part of their length are overexposed along another part of their length. Thus it becomes a Herculean task to obtain quantitative

information about line intensities or variation in line intensity along the path as seen in a particular wavelength.

These spectrograms illustrate another unavoidable feature of the beam-foil source. You will note that the lines in the bottom picture, taken at 2 MeV, show quite a slant towards the long wavelength end of the scale relative to what one sees in the top picture at 0.5 MeV. This slant originates from the Doppler effect, which has serious consequences for beam-foil spectroscopy.

Figure 4 illustrates the origin of this characteristic. Here we see H_α at 6563 Å from a rather long length of the beam.[2] The optical system sees the light which comes from points close to the foil as blue-shifted, while points far downstream give light which is red-shifted. In the case which is displayed, the total shift from one end of the line to the other is some 20 Å. This is rather extreme, in that quite a long length of beam is involved. The fact is that every finite length of beam gives rise to this Doppler shift from one end to the other. If one looks at a short beam segment, the line is Doppler-broadened.

Another source of Doppler broadening is illustrated in Fig. 5. Here we see that the finite acceptance aperture of the optical device introduces a Doppler broadening even for light which comes from a single point on the beam. In practical terms, the Doppler broadening for wavelengths in the vicinity of 5000 Å can easily be 10 Å, a situation which is clearly intolerable if one is to do

spectroscopy with any reasonable degree of precision. We will see in a moment that it is possible to remove these gross Doppler effects and thereby obtain fairly good line shapes, but two residual problems remain. One is that scattering by the foil or any other source of divergence or convergence of the luminous beam introduces an inescapable Doppler broadening. The other is that if one does not know the viewing geometry with respect to the beam to high precision, and one rarely knows that, one can introduce Doppler shifts of the spectral line even if there isn't any broadening. Such shifts complicate calibration of the spectrometer and the identification of the spectral lines.

Stoner and Leavitt[3-5] introduced a clever method of compensating for the Doppler broadening that has an origin in the finite length of beam which is viewed. In Fig. 6 we show a grating which is illuminated by light from either a fixed source or a moving source. Light rays from the fixed source follow the solid lines to the grating and then to a focus in the exit plane of the instrument. However, if the source of light is moving, an emitter which is on the upstream side of the entrance slit looks to the spectrometer as though it is too blue and it therefore follows the dashed line marked "B". However, if the light comes from the downstream side of the beam it looks too red, and it follows the dashed line marked "R". What we see is that these light rays have a new focus which differs from the position of the conventional focus. Stoner and

Leavitt calculated the amount by which the exit slit has to be moved to compensate for this particular Doppler effect and some results are shown in Fig. 7.

In Fig. 7, see data taken with a 4 MeV beam of nitrogen.[3] The lines under investigation come from N IV, or three times ionized nitrogen, in the vicinity of 3500 Å. The open circles show the kind of data that we were taking prior to the application of the Stoner-Leavitt refocusing compensation. The solid dots show the clear advantage of moving the exit slit to a point which is appropriate to the speed of the emitters and the wavelengths of the light being detected.

Still another Stoner-Leavitt method,[6] shown in Fig. 8, permits one to reduce the effect of the finite entrance aperture into the spectrometer. Here we have a lens between the beam and the entrance slit. The focal length of the lens is so selected that the red-shifted or blue-shifted light is refracted by just enough to have the rays which leave the grating travel along the same path as the central ray. Using this intensity enhancement idea, we obtain results such as appear in Fig. 9.

We look again at those lines in nitrogen which we saw a moment ago. With the conventional arrangement, we get the upper pattern. With an intensity-enhancement lens in place, we see the lower pattern. Now the linewidth in the lower pattern is not so good as in the upper part, but I call your attention to the fact that the same running time with the same beam strength gave a peak intensity of

almost 4000 counts in contrast to the 160 or 170 counts from the conventional geometry. Thus the line intensity has been enhanced by a factor of about 20 at some cost in line width. Since there are many cases where the lines are isolated but still weak, intensity enhancement can be quite useful. Of course one is restricted to the wavelength range where a lens can be used, which means a practical lower limit in the neighborhood of 2000 Å.

Early in this paper, I pointed out that one of the advantages of the beam-foil source is that one can see light from a number of different stages of ionization of an element. A disadvantage, however, is that several stages of ionization are present at the same time, so that one has to find a way of associating a given spectral line with the particular stage of ionization from which it comes. To do so, we make use of the fact that the target chamber is at ground electrical potential, which makes it simple to subject the radiating beam to an external electric field. If the field is transverse to the beam velocity, the beam is deflected sideways by an amount which depends upon the charge on the particle. An early example of this work[7] appears in Fig. 10. Here a collimated beam of nitrogen with an energy of 2 MeV is deflected to the side by a transverse field of 75 kV/cm. The beam is very clearly split into two, the upper one consisting of absolutely pure singly-ionized nitrogen, the lower one being a beam of doubly-ionized nitrogen. If one then does spectroscopy on those separated beams, there is no

question as to the stage of ionization from which the observed wavelengths come.

Figure 11 shows the first data that were ever obtained in this fashion.[7] Again we used a Meinel spectrograph, which was so arranged that light from beams that were not deflected very much appeared towards the top of the photograph whereas light which came from beams with greater deflection showed at lower points on the plate. We see a clear separation of spectral lines coming from N II, III, and IV. We have also used several modifications of this basic method. In the one used most recently,[8] we employed a spectrometer, but took advantage of the fact that there is a spatial separation of the beams of light in the exit plane of the spectrometer just as there is in the entrance plane. We can then move a small slit along the exit aperture and pick up light from different positions, which permits us to determine the charge of the emitter. As of this point our greatest success has been with identifying light from ten-times ionized krypton.[8] That approach tends to be a bit time consuming, but I think that we can simply cover the exit slit with a position-sensitive detector which has good spatial resolution and thereby reduce the labor by quite a bit.

A related method[9] is shown in Fig. 12. Here the beam is deflected toward or away from the spectrometer so that there is a Doppler shift which is proportional to the charge on the emitter. Some data appear[10] in Fig. 13, where we see the wavelength shift of

a line from N IV. You will notice that the shifts are not quite symmetric for the red and blue cases. This is the result of changing the detector geometry when the beam is deflected towards or away from the spectrometer.

One last example of this kind of work is shown in Fig. 14, where we see some data from krypton.[10] These lines originate in Kr VIII and X, that is 7 and 9 times ionized krypton, respectively. While the shifts are large, one also sees that the intensities are strongly affected by the application of the field. That comes about because the particular spectral lines which you see are mixtures of ℓ-states; they are subject to a special effect which I will discuss later on in quite a different connection. Despite that effect, which takes place only for states with rather large principal quantum numbers, one can still determine the appropriate stage of ionization.

Now we have seen that the photographic recording technique has such limitations that the spectrograph has been largely supplanted by the spectrometer. Nonetheless, we also saw that the spectrogram allows one to see many things at once, whereas the spectrometer is restricted to giving information on a single spectral line or a small piece of radiating beam for any one measurement. I want to conclude this first part of my talk by showing two more figures based on data taken with a Meinel spectrograph.

Figure 15 shows some spectral lines from neutral and singly ionized helium.[11] What you will notice is that the lines at 5412, 4859, and 4541 Å exhibit a peculiar behavior. They show a distinct break in intensity along their lengths. Those breaks do not occur at the same positions downstream from the foil, nor do they have the same length. It appears, in fact, that the excited atoms or ions giving these spectral lines simply ceased radiating, and then began to radiate again a little further downstream. The patterns which appear in Fig. 16, and which also come from helium, are even more striking in this regard.[12] Here the lines at 4859, 4541, and 4388 Å all show repetitive patterns of bright and dark regions. These effects have to do with the quantum-mechanical interference of short-lived and long-lived components of the parent spectroscopic terms, in these instances, under the influence of a small external electric field. These were some of the early observations of the general phenomenon of quantum beats which Andrä will discuss in his paper. I will say nothing further about these patterns except to point out that the qualitative nature of the data obtained with a spectrograph can sometimes be far more illuminating of a complex situation than the quantitatively more satisfying data which one can collect with a spectrometer.

Let me now turn from this historical survey of beam-foil spectroscopy to some of the modern quantitative results on optical spectra and the structure of ions. I have already shown a few

spectra from hydrogen, helium, nitrogen, and krypton. Let me illustrate further the versatility of the beam-foil source by showing data obtained in various laboratories from a variety of elements.

Figure 17 shows chromium energized to 230 KeV and observed in the near ultraviolet.[13] There are 15 or so quite distinct lines which are identified as coming from the singly-ionized system. This illustrates one of the handicaps of the beam-foil source. Although the particle velocity is low in this instance, there are no lines, or at least no strong lines, from the neutral atom. Consequently, it becomes quite difficult to make any observations on the neutral species although, of course, neutral atoms are of the greatest interest in many different phases of physics. If one should lower the bombarding energy so as to enhance the production of neutrals, one faces the problem that the particle energy loss in the foils gets so large that the foils tend to break before one can get much useful information.

Figure 18 shows some data taken on lead.[14] In this case we were actually able to observe lines from the neutral species, so it is not completely impossible to observe neutrals. Some of these lines are of particular interest because they are the same ones seen by astronomers who look at the sun and from the intensities of which the abundance of lead in the sun is determined. Our intention was to measure the lifetimes of the parent levels, but this requires knowing the particle velocity. For the case of these neutrals we were merely able to estimate the energy loss in the

foils but that is a very poor way of getting at the number of interest. Consequently, we do not consider that the lifetime values we obtained were particularly reliable. Our suspicion of those numbers was intensified when we found that we got the same solar abundance of lead as the astronomers did.

Numerous other metallic elements have been used in beam-foil work. In a recent paper, Martinson[15] mentions some 60 elements, including Li, Be, C, Na, Mg, Al, Si, K, Ca, Sc, Fe, Ni, Pb, and Bi. Many of the rare earths have been studied,[16-19] as well as[20] Se, Ge, As, Sn, Sb, and Te.

In Fig. 19 we see some more data[21] for the element krypton. Here the particle energy was 2 MeV and the normal-incidence spectrometer was refocused so as to give the best line width permitted by the beam-foil source. As you can see, that line width is 1.4 Å, which is not very good in terms of classical optical spectroscopy. There are a number of unresolved regions in this spectrum, and it remains one of the most refractory of tasks for the beam-foil community to learn how to resolve this type of structure. You will notice also that there are identified lines from Kr VI and Kr IX, that is to say, 5 and 8 times ionized krypton, respectively. The identifications, however, do not contain any detailed spectroscopic information, but simply indicate the principal quantum numbers of the levels between which the transitions occurred. These so-called "Rydberg lines" have considerable importance, and I will talk about them at length in the next part of this discussion.

Figure 20 shows some more krypton data,[21] this time taken with 5 MeV particles. Here the stage of ionization has gone up to 9+. Unfortunately, the line width has also increased, since we are here in a longer wavelength regime than in the previous work. Again we see that the transitions are specified only in terms of the principal quantum numbers of the connecting levels.

In Fig. 21 we see about the most careful spectroscopic work that has been done in the visible part of the spectrum;[21] the limitation on the quality of the spectroscopic data is quite obvious. The problems of wavelength resolution become much simpler at the short wavelength end of the spectrum. This is because the Doppler effect is roughly proportional to the wavelength.

In Fig. 22 we see some data taken[22] with a home-built grazing-incidence spectrometer on the element oxygen. The wavelengths are now in the vicinity of a couple of hundred angstroms. You see that the line width is down to 1.2 Å which is not very good, but, in this case, results from the design of the spectrometer itself rather than from the Doppler effect. In fact, in some other work on silicon discussed below,[23] it has been possible to obtain a line width of only 0.15 Å in the grazing-incidence region.

Two other features of Fig. 22 deserve mention. One is that the relative intensities of the lines cannot be accounted for at the present time. We have absolutely no idea as to why some transitions are prominent and others not, either in this spectrum or in any

other. The other feature is that here at 5 MeV with oxygen we could produce charge 5+, that is to say O VI. Just a moment ago, however, we saw that 5 MeV krypton gave us Kr IX. It becomes increasingly difficult to remove the inner electrons of even the light elements, although it is fairly simple to strip off a large number of electrons from the heavy elements. Figure 23 also shows this effect. It is a sample of data[22] from fluorine at 4 MeV. We see several lines from F VII, the lithium-like structure, just as O VI represented three-electron oxygen. However, the helium-like system cannot be excited at this bombarding energy.

Fluorine shows a veritable forest of lines in the extreme vacuum ultraviolet and it is clear that there is a great wealth of data which can be explored. For argon,[22] which we see in Fig. 24, the spectrum is so rich in lines that wavelength resolution is once again starting to be a serious problem.

Transitions with short wavelengths differ in an important respect from those at long wavelength. The short lines link states the lower of which are close to the ground term. Consequently, one now has the opportunity to determine real spectroscopic information about the excited system, whereas the lines of long wavelength tend to connect only Rydberg levels.

Figure 25 shows some silicon data taken with quite high spectroscopic resolution, again in the grazing-incidence region.[23] Working at 20 and 42 MeV, we were able to associate many of our

lines with high-resolution data obtained with standard spectroscopic sources. The very strong Si X line at 348 Å is prominent in the solar corona and comes from a ^2D-$^2D^o$ configuration. The weak features around 360 Å remain unidentified. The very strong line in Fig. 25 and the one to the right, unfortunately taken with different resolving powers, are quite interesting in that they come from sodium-like iron, that is, 11-electron iron. They are, in fact, the sodium D-lines, but instead of occurring at 5890 and 5896 Å as in the case for neutral sodium, we find them in the vicinity of 350 Å.

Figure 26 shows some data obtained on copper at two different bombarding energies.[24] The spectrometer used in this experiment was a Seya-Namioka, which gave us a line width of 15 Å. Of course you can cover a lot of territory within 15 Å. Nonetheless one sees that there are a great number of discrete spectral features and that there are significant changes in the spectrum as one goes from 16 to 30 MeV, even though the change in particle velocity is only 40%. Copper was a nice element to work with because the beam intensity was high and the wavelength regions we explored were largely unknown to spectroscopy. It is very inviting to think of returning to this element with a better spectrometer.[25]

Figure 27 shows similar data[24] for iron at two different energies. I display this primarily to show the great range of particle energies over which beam-foil experiments are now being

conducted. In Fig. 28 we see some additional work on iron[26] but in a shorter wavelength region and with much better resolving power than was used on the other experiment. Here at 35 MeV we see that we have identified lines coming from Fe XVI, that is, 15 times ionized iron, whereas Fig. 25 on silicon at 40 MeV showed only Si X. Again we see that the more complicated the element the easier it is to strip off and excite many of the outer electrons.

Figure 29 illustrates the best resolving power that we were able to use for the case of iron, the principal limitation here being that the beam was quite low. It was only about 10% of the copper beam for example, and we frequently dealt with less than a particle nanoamp. While it is encouraging that one can get data with such small currents, it is obvious that one could do much better with better ion sources for the accelerators.

Now I mentioned earlier that a lot of the spectral features originate in states of rather large principal quantum number. The orbits for the electrons are all so large that all the electron sees is the Coulomb field of the core. Consequently, the states and the transitions are essentially independent of the specific nature of the element or ion and the system behaves like the Bohr model of the hydrogen atom. Among other things, this means that the spectral distributions look pretty much the same as one goes from element to element. A good example[24] appears in Fig. 30. Here we display 16 MeV copper and iron. Although there are a few

differences in relative intensities in these patterns, it is clear that there is a striking identity. Most of these lines are the so-called "Rydberg lines", which correspond to electron jumps of 1 or 2 units of principal quantum number. Figure 31 shows[24] a similar comparison for iron and copper but in a shorter wavelength region. Here we find that the spectra start to exhibit differences, along with some similarities. The differences, of course, reflect the specific character of the iron or the copper, whereas the similarities are indicative only of Rydberg transitions.

Figure 32 summarizes our preliminary results[24] on the structure of iron. On the left hand part of Fig. 32, we have drawn the transitions with $\Delta n = 1$ which we detected; it is comforting to note that if we made the claim that we saw the 12 to 11 jump, we also saw 11 to 10, and so forth, all the way on down the line within the wavelength range of our experiment. In the middle portion of Fig. 32 we see the $\Delta n = 2$ transitions and, at the right, there are $\Delta n = 3$ lines.

Clearly, the beam-foil source populates levels with fairly high values of principal quantum number. We have seen in the example of iron that the spectral data are useful for providing information about the level structures of various stages of ionization. Of course in the work shown on iron, the levels themselves were not particularly interesting because they were levels with very large values of n and therefore did not contain any detailed information about the electronic systems. In other cases, especially for the

lighter elements, we have found it possible to construct level schemes where none was previously known. For example, Fig. 33 shows the case[27] of Cl VII. The spectral lines which are shown on the slide are those we detected in the beam-foil experiments. It is worth pointing out that only the two lowest of these lines had ever been seen in other kinds of spectroscopic work on chlorine. This entire level scheme was then constructed on the basis of our observations and calculations. A similar level scheme is shown in Fig. 34 for the case[28-30] of S VI. Thus it is quite apparent that the beam-foil source can play an important part in clarifying the level scheme for multiply-ionized systems which have previously been explored only rather incompletely, if at all.

As one goes through the calculations which transform the observed wavelengths into the positions of levels, one finds that there are various correction factors which have to be incorporated into the calculations because there may be polarization of the core or shielding factors which introduce deviations from a simple Coulomb field. Thus the level positions vary as one goes along an isoelectronic sequence. Figure 35 shows the smooth behavior[15] of certain levels in the Mg I sequence. Since this kind of reduction of the data must be carried out for all terms in all isoelectronic sequences, you can see that the total amount of labor involved is enormous.

Up to now, I have discussed only rather ordinary kinds of transitions. However, the beam-foil source populates kinds of

levels which rarely make their appearance in other light sources. These levels make their presence known in terms of spectral lines which cannot be fitted into a standard level scheme. An example appears in Fig. 36 where we see the spectrum of lithium.[31] The lines which are labeled with the letters A, B, C, and D and which are quite strong cannot be accounted for in terms of the ordinary level structure of lithium. However, one can explain these lines in terms of transitions between levels in which two electrons are simultaneously excited. Because the beam-foil source is a prolific generator of these multiply-excited systems, a lot of attention has been paid to them. Figure 37 shows the structure[32-34] for the two-electron, doubly-excited system in helium. You will notice that the lowest term in this picture is considerably above the ionization level for helium, but there are still many discrete states which are connected by the spectral lines. This situation is quite familiar in nuclear physics, where one has countless discrete states well above the energy at which one or more particles can be evaporated from the nucleus and whose presence is detected, for example, by gamma rays which connect these high-lying states to lower ones. It is, however, surprising to find that the Coulomb field, which is far weaker than the nuclear field, also accommodates a large number of bound structures well above the ionization limit.

I come now to the measurement of a lifetime. As you know, the method is to set the spectrometer on a single spectral line and to

measure the intensity of that line as a function of distance downstream from the excited foil. An example of the data one can obtain[35] is shown in Fig. 38. The intensity of this line in Be II is plotted on a semi-log scale; over a range of about a factor of 50 in intensity, the decay is quite exponential in character. From the slope of this line and the known particle velocity, one deduces the mean life of the parent level, which, in this case, is about two nanoseconds. I might remark in passing that, using the beam-foil source, my colleagues and I measured the first lifetime ever obtained when the associated radiation was in the vacuum ultraviolet and also the first for which the radiating system was multiply-ionized.[36] These substantial achievements should be kept in mind as I proceed to talk about some of the problems that are associated with the deduction of lifetimes from measured decay curves.

Among the problems one encounters is the non-linearity of the decay curve on a semi-log plot. The situation is nicely illustrated in Fig. 39, where, in (a), we see a very good exponential decay[36A] curve from 0 V. Here, the observed range of intensities was over a factor of 20. In Fig. 39 (b) is a different case.[37] Here there is a fair amount of curvature in the early part of the decay curve, and, in fact, the curvature is concave downward. This behavior is interpreted as originating in a feeding of the level which is under direct observation by cascade from a higher level. Moreover, the

higher level actually has a shorter lifetime than the one being studied. Usually, the lifetimes get longer as one goes to higher and higher excitation; the effect of this appears in Fig. 39 (c), where we see curvature that is concave upwards and is attributed to cascades.[38]

By decomposing the data into a sum of exponentials and also accounting for background, one can determine the mean lives of the cascading level or levels, as well as the mean life of the level being observed. Although that procedure is straightforward it is not unambiguous. For example, Fig. 40 shows some decay data[39] for Ti II. On the right we see two different decay curves for a particular level. These decay curves were taken with different velocities so as to make sure that the curves scale properly. They do indeed, and these straight line decays give a lifetime of about 7 nanoseconds for this particular level. On the left, we see the decay curve for another level in Ti II; here there is marked curvature. The standard interpretation of this figure is that the level in question was populated by cascade from a higher level. However, I believe that there is good reason to doubt this interpretation of the curvature.

If we look at Fig. 41 we see the level scheme for Ti II. The level labeled z $^4G^o$ is the one for which the decay was clearly exponential. However, this level is also fed by cascade from at least one higher level. On the other hand, the e ^4G term, which is quite

close to the ionization level and into which there is hardly any level at all that could cascade, is the one which shows the curvature! Consequently, it seems to me to be wrong to interpret the curvature of the intensity variation as coming from cascades. Moreover, the fact that a level into which cascades are known to take place actually exhibits an exponential decay suggests that where cascades occur in fact they are of little significance. A similar situation, even more striking, is illustrated in Fig. 42. Here we show a low-lying level in N V. It is fed by cascades from at least a dozen other terms, but, as you can see from the decay data[40] which appear in the figure, the decay curve is quite exponential. On the other hand, the high-lying level indicated in the figure gives decay data which exhibit considerable curvature.

Still another example appears in Fig. 43. The upper curve[41] is from the decay of a low-lying term in S IV; it is strictly exponential over an intensity range of about a factor of 10. On the other hand, the marked curvature of the bottom curve comes from a transition which Martinson[42] has just identified as coming from a high-lying level of S V; this curvature is just like that of the other terms we saw in the previous examples for which curvature was so apparent.

If we consider the nature of those high-lying levels, recall that they are Rydberg levels. That is to say, they are characterized by a principal quantum number, and contain a large number of

quasi-degenerate states having different ℓ-values. As a result, what the spectroscopy gives is a blend of very closely spaced lines coming from levels with a large number of different lifetimes. It is my belief that the curvature which characterizes these high-lying terms comes simply from this mixture of ℓ-states, that is to say, a blend of the spectral lines that are associated with the decays of the individual ℓ-states, rather than from cascades.

Now it is one thing to make a suggestion of this nature and it is another to give quantitative evidence that the suggestion is correct. We have carried out two different kinds of investigations in order to clarify the situation. In the first instance, I pointed out that if there truly is a mixture of ℓ-states with various lifetimes, the application of a small electric field would introduce Stark mixing of those levels. Therefore, what Condon and Shortley refer to as the average mean life of the term would be markedly reduced. The idea then is that one observe the intensity of one of these spectral lines with and without an external field. If there is Stark mixing of any ℓ-degenerate levels, the intensity of the line should be markedly affected by the presence of the field. Now whether the line intensity declines or increases depends on such factors as the speed of the beam, where one looks relative to the excited foil, the strength of the electric field, and the intrinsic character of the level, but the point is that a field-dependent intensity is sufficient evidence that the level is a Rydberg level.

The first data along these lines were taken by Jack Leavitt[43] of the Arizona Laboratory. He applied an electric field parallel to the beam so as to avoid any geometrical effects that would occur from bending of the beam towards or away from the spectrometer. Some of his results appear in Fig. 44. On the upper part of Fig. 44 we see some spectral lines in neon. The very strong line had been previously identified as being a Rydberg line coming from transitions between n = 8 and n = 7. The upper part of the figure represents data taken in the absence of an electric field. On the lower part, we see the result of putting on an electric field of about 30 kV/cm. It is immediately obvious that that strong Rydberg line has been quenched relative to the other lines in this part of the spectrum; it is therefore shown without any question that there is ℓ-degeneracy, that there is Stark mixing, and that any decay curve taken on this particular line must show curvature. That curvature, however, has absolutely nothing to do with feeding of the level of interest by cascade.

Similar work has been done by Leavitt[44] on krypton and oxygen and in every case where the term was of the Rydberg character, this phenomenon of quenching was displayed. This, I believe, truly accounts for most of the curvature seen in beam-foil lifetime data.

That is not to say, of course, that cascading never occurs. It obviously occurs for low-lying levels. Just by way of example, we have seen the Lyman lines in hydrogen and also the Balmer lines;

that is proof enough that there is cascading. However, the fact seems to be that a cascade contribution to a decaying term is so small, partly because the population of the upper level is less than that of the lower term, and partly because the relative lifetimes of the two terms are quite different, that the influence of cascades is almost negligible.

Leavitt and Dietrich also carried out a different type of attack on this problem of cascades.[45] They used the technique of refocusing[3,4] so as to get as narrow a line shape as possible. They considered a system, N V, for which they could resolve the various ℓ-states and for which there are good calculations of level lifetimes. They then made standard type observations on the decay curves, sometimes on these resolved lines and sometimes on lines which resulted from a deliberate blending of levels. That blending is easily accomplished just by opening the spectrometer slits a little bit. Figure 45 shows one result. Here we see the decay of a level excited with 5 MeV nitrogen. The line intensity was followed over a range of about a factor of 100 and impeccable data were obtained at every point along the curve. This curve was then treated as a sum of exponentials; the primary and two secondary lifetimes were determined. In Fig. 46, we have a summary of the cases which were investigated. For these nine successive values of n and some 30 different ℓ-states in all, measurements were made with the care displayed on that previous slide. At each place

where an X appears, a measurement was made. Two or three X's mean that there were two or three different modes of decay, each of which was observed independently and from which a lifetime was found. The numbers on these particular levels are the theoretical lifetimes as calculated according to the Coulomb approximation.

Figure 47 summarizes some of the results. Let us look, for example, at the 6 F level, which was seen in decays to both 5 D and 4 D. You see that the lifetime, measured from the 6 S to 5 D transition, was found to be 0.41 nanoseconds, whereas it was 0.46 nanoseconds in the 6 F → 4 D decay. These values are in good agreement within the experimental errors, and they compare not too badly with the theoretical value. The experimental number is a bit longer than the theoretical number but that is not an uncharacteristic result of this type of experiment. Now let us take a look at the 6 G lifetime, which is found to be 0.72 nanoseconds, in comparison with the theoretical calculation of 0.64 nanoseconds. Again, the agreement is not too bad. If, however, we open the slits, the light from the 6 F and 6 G levels, with wavelengths which differ by only 1.5 Å, is accepted by the spectrometer as a single line. Then one has this last entry of 4DF - 6FG, and one gets a so-called "lifetime" of 0.67 nanoseconds. Also, the decay data are quite curved, with an apparent cascade contribution with a lifetime of 0.51 nanoseconds. Thus it is clear that these numbers from blended lines have little physical significance. It is safe to conclude from these studies

that curvature to any significant degree is almost certainly associated with Rydberg terms where there is degeneracy and that the so-called "lifetimes" that are found from such curves are not very useful. On the other hand, Leavitt did find that there might still be some curvature for isolated lines because one does at least have background. There is also some cascading, of course. However, for the isolated lines, the lifetimes which are found from the early part of the decay curves are quite respectable. Figure 48 is a summary of the lifetime measurements for the 30 or so different terms investigated in this very careful experiment.

Still another interesting result came from this particular work. One can adopt a model which describes how levels are excited. A popular model, for example, is one in which the level population falls off as n^{-3}. One can then use, let us say, "theoretical lifetimes", in order to construct the decay curve for some particular level. One can then compare that decay curve with an observed decay curve to see whether the model gives agreement with the data. Figure 49 shows just such a comparison. The upper curve has been calculated on the assumption that the level population falls off as n^{-3}, whereas the lower curve shows the experimental result. It is apparent that the n^{-3} distribution gives a much larger contribution to the cascading process than is actually observed. Therefore, we can conclude from this experiment that the level population declines faster than n^{-3} and it must be at least

partly for this reason that the cascade contributions, where they do exist, are relatively small and unimportant.

There are a number of different applications for the lifetime experiments. It is often convenient to talk not in terms of lifetime or transition probability but oscillator strength, a quantity which is directly proportional to the transition probability. Various workers like Sinanoğlu, Andy Weiss, Wiese, and others have calculated oscillator strengths as a function of position along an isoelectronic sequence. This has been done for many different types of transitions. Wiese[46] and his associates in particular have shown that these oscillator strengths exhibit smooth variations with Z so that one can interpolate or extrapolate into regions where neither calculations nor experiments have been carried out. However, it is necessary to do a fair amount of work in order to establish the particular kind of trend.

Figure 50, for example, shows an interesting case[46] in the B I sequence. In the vicinity of carbon, there is destructive interference between two levels. This gives a decrease in the oscillator strength, so that there is a dip in the curve. A different case[46] is shown in Fig. 51, where there is an obvious maximum to the curve. I might say that practically all of the data in Figs. 50 and 51 comes from beam-foil experiments.

Figure 52 shows[46] a much smoother dependence on Z with neither a maximum nor a minimum. Figure 53 illustrates[46] very nicely the importance of experiment, because here we have several different kinds of calculations. The experimental values show that only one

kind of theory is suitable for accounting for this particular variation of oscillator strength with Z.

There is another important application of lifetime data, to quantum electrodynamics. In that field Marrus and his colleagues[47] have worked on the decays in 1 and 2 electron systems of very high Z. They have seen a variety of forbidden decays, and, in general, have measured lifetimes in agreement with QED. However, there is an anomaly for the cases of $C\ell^{15+}$ and Ar^{16+}. Still another application of lifetime data is to determine the abundance of the elements in the Galaxy. A most important contribution in the latter case has been the work on iron, where it was shown[48] that the iron abundance in the sun is actually some ten times greater than was thought to be the case on the basis of oscillator strengths derived from standard spectroscopic experiments. Finally, lifetime measurements have considerable significance, even for light elements but especially for the metals, in connection with the operation of hot plasmas in controlled thermonulcear reactors, the reason being that such elements are contaminants which adversely affect plasma behavior.

Problems for the immediate future include finding a way of narrowing the line widths so that better spectroscopy can be done with the beam-foil source. A possible way of doing this is to cross the ion beam with a laser, and to use Doppler tuning to bring the laser line into coincidence with the transition wavelength between a level in the beam and some higher one. Presumably one could thereby eliminate all the effects of Doppler broadening.

A second problem is to improve the lifetime determinations, and, especially, to find out to what extent the measurements are affected by cascades. This, too, could be approached with laser excitation, for one would then be able to excite some level without having it repopulated from higher terms.

Thirdly, one would like to extend measurements to highly-ionized metal atoms so as to provide numbers of interest in the CTR work. At the same time, one opens the possibility of looking at relativistic effects in the level structures and decay probabilities in such systems.

A great deal remains to be done towards understanding the beam-foil interaction, especially from the theoretical side. As noted in my paper, there is now no way of accounting for relative line intensities. Finally, there are prospects for observing Zeeman splittings and for measuring hyperfine-structure separations.

FIGURE CAPTIONS

1. Experimental arrangement for beam-foil work. A Meinel spectrograph is indicated as the optical analyzer.
2. A beam of nitrogen, with an energy of 2 MeV, moves from right to left. The interior of the target chamber is viewed through a transparent window. The vertical streak of light is reflected from the foil holder; the horizontal streak is from the particle beam, rendered self-luminous by its passage through the carbon foil.
3. Three spectrograms of nitrogen at different particle energies. a (top): 0.5 MeV; b (middle): 1.0 MeV; c (bottom): 2.0 MeV.
4. Origin of Doppler slant of spectral lines. The beam was hydrogen. The line displayed is H_α.
5. Doppler broadening from the finite acceptance angle of the spectrometer.
6. Illustration of refocusing.
7. Results of refocusing. The lines are from N IV, generated with 4 MeV N.
8. Method of intensity-enhancement.
9. Intensity-enhancement data.
10. Field-separated beams of N^+ and N^{2+} to identify charge-states.
11. Result of spectroscopic study, with a Meinel spectrograph, of field-separated beams of N^+, N^{2+}, and N^{3+}.

12. Illustration of Doppler-shift method of identifying charge states.
13. Doppler-shift data for identifying charge states.
14. Another example of Doppler-shifted data for identifying charge states.
15. Spectrogram of He, showing "breaks" in certain spectral lines.
16. Field-induced quantum beats in He II spectral lines.
17. Beam-foil spectrum of 230 keV Cr.
18. Beam-foil spectrum of Pb at low energy.
19. Beam-foil spectrum of 2 MeV Kr.
20. Beam-foil spectrum of 5 MeV Kr.
21. Example of "high-resolution" beam-foil spectroscopy on Kr.
22. Beam-foil spectrum of oxygen, observed in the region of grazing-incidence.
23. As in Fig. 22, but for fluorine.
24. As in Fig. 22, but for argon.
25. High resolution spectrum of 40 MeV silicon in the grazing-incidence region.
26. Beam-foil spectra of Cu at 16 and 30 MeV. Here the line width was 15 Å.
27. As in Fig. 26, but for Fe at 16 and 110 MeV.
28. As in Fig. 27 in a different wavelength region.
29. High-resolution spectrum of 35 MeV Fe.
30. Comparison of 16 MeV Cu and Fe spectra.

31. As in Fig. 30 in a different wavelength region.
32. Summary of preliminary analysis of Fe data, indicating a large number of Rydberg transitions were seen.
33. Level structure of Cℓ VII, as deduced from beam-foil spectroscopy.
34. As in Fig. 33, but for S VI.
35. Variation with Z of some level energies along Mg I isoelectronic sequence.
36. Beam-foil spectrum of Li. The letters indicate lines from transitions originating from doubly-excited levels.
37. Levels of doubly-excited He.
38. Beam-foil decay data for a line in Be II.
39. Examples of decay data seen in beam-foil work.
    a) exponential
    b) cascade effect where cascade contributor is shorter-lived than level of interest
    c) cascade effect where cascade contributor is longer-lived than level of interest
40. Decay data for different levels in Ti II.
41. Level scheme for Ti II.
42. Level scheme and some decay data for N V.
43. Decay data from (a) S IV and (b) S V.
44. Beam-foil spectra of Ne, (a) without applied field, (b) with applied field.

45. Decay data for a line in N V.

46. Summary of levels in N V studied by Leavitt and Dietrich.[45]

47. Preliminary analysis of some of the decays in N V.

48. Summary of preliminary lifetime results for N V.

49. Comparison of decay curves as expected from n^{-3} excitation dependence and as observed.

50. Variation of oscillator strength of a transition in the B I isoelectronic sequence. Destructive interference occurs near C II. Symbols from experiments.

51. As in Fig. 50, but showing a maximum near C II. Solid symbols and X's are from experiments.

52. As in Fig. 50, but for Li I sequence. The behavior is monatomic with 1/Z. Solid symbols from experiments.

53. As in Fig. 50, but comparing various calculations (open symbols) with experiment (solid symbols). Δ, self-consistent field; O, superposition of configurations; □, two-configuration approximations.

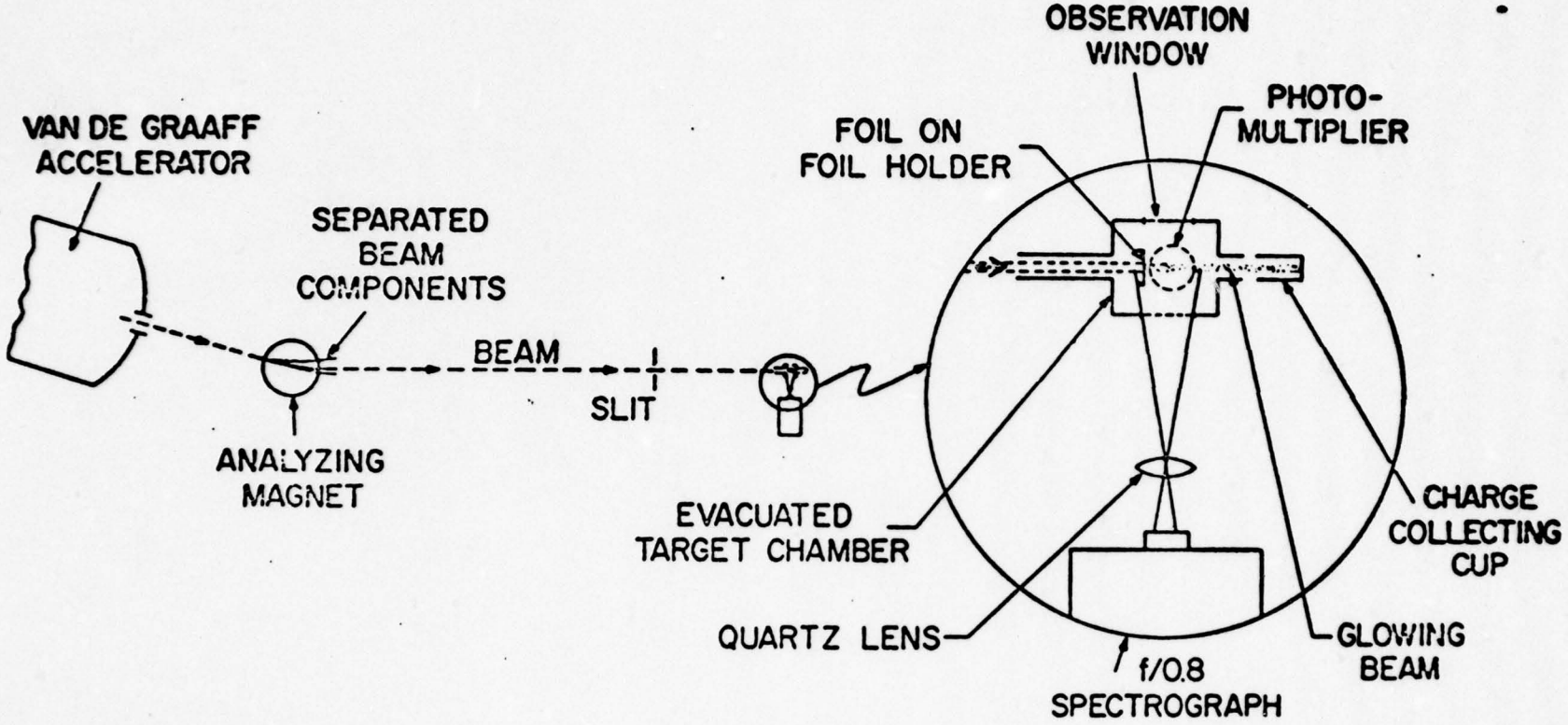
OBSERVATION WINDOW
PHOTO-MULTIPLIER
FOIL ON FOIL HOLDER
VAN DE GRAAFF ACCELERATOR
SEPARATED BEAM COMPONENTS
BEAM
SLIT
ANALYZING MAGNET
EVACUATED TARGET CHAMBER
CHARGE COLLECTING CUP
QUARTZ LENS
GLOWING BEAM
f/0.8 SPECTROGRAPH

Fig. 1

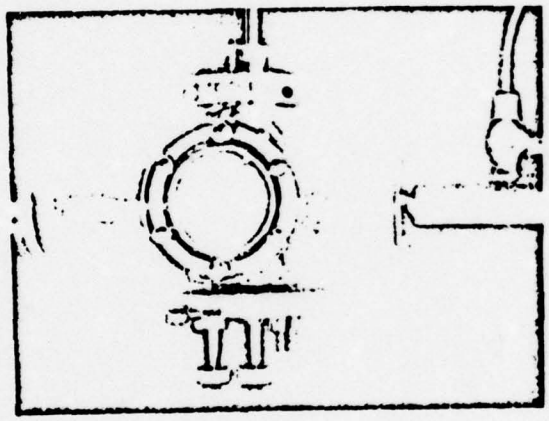

Fig. 2

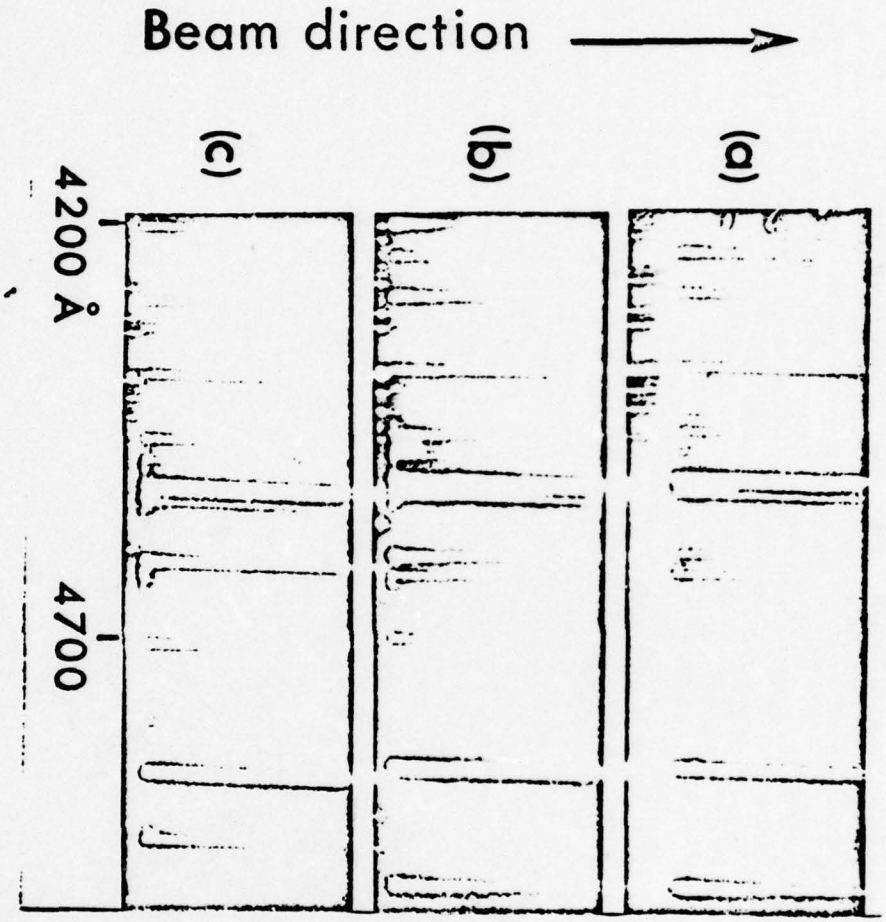

Fig. 3

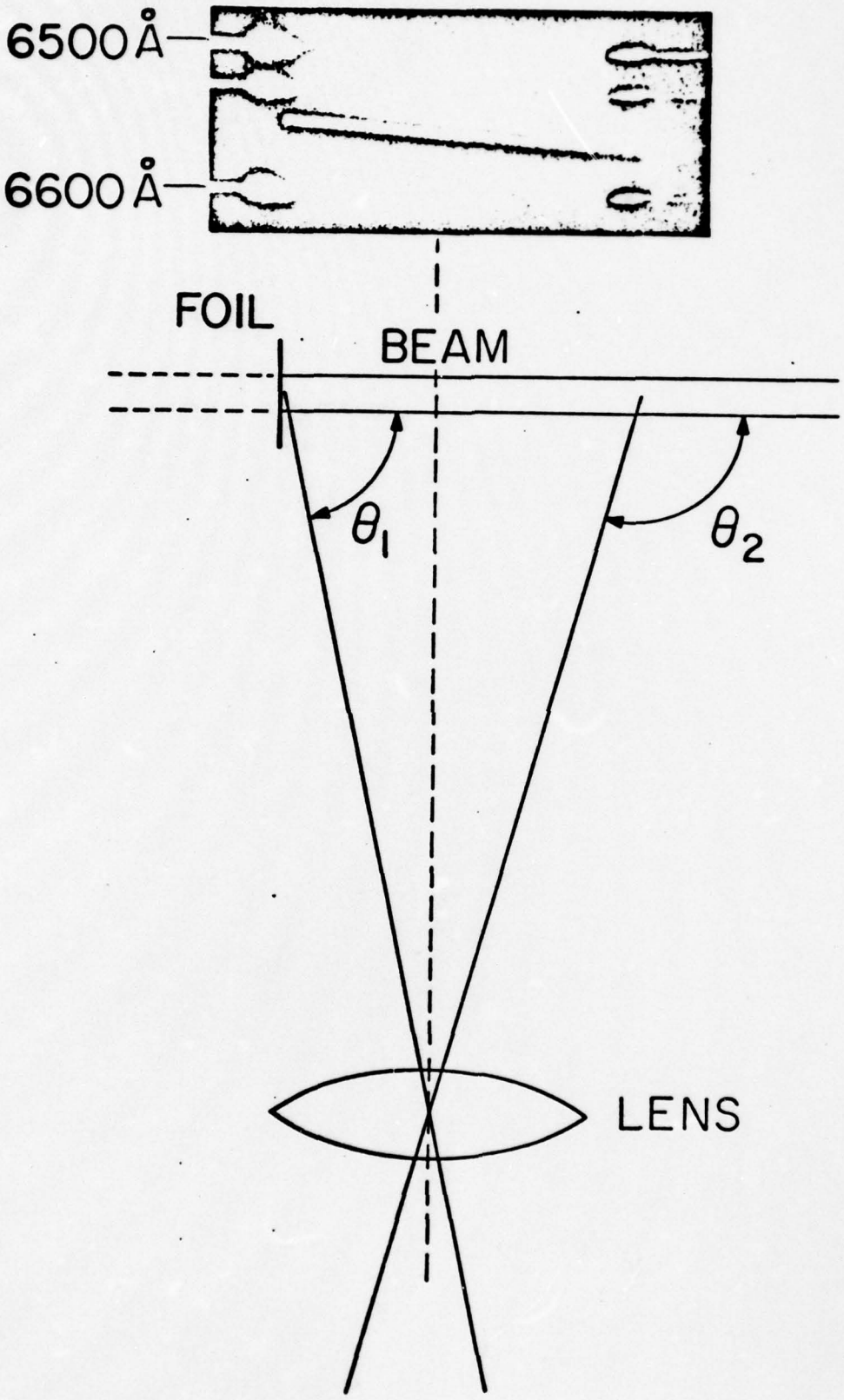

Fig. 4

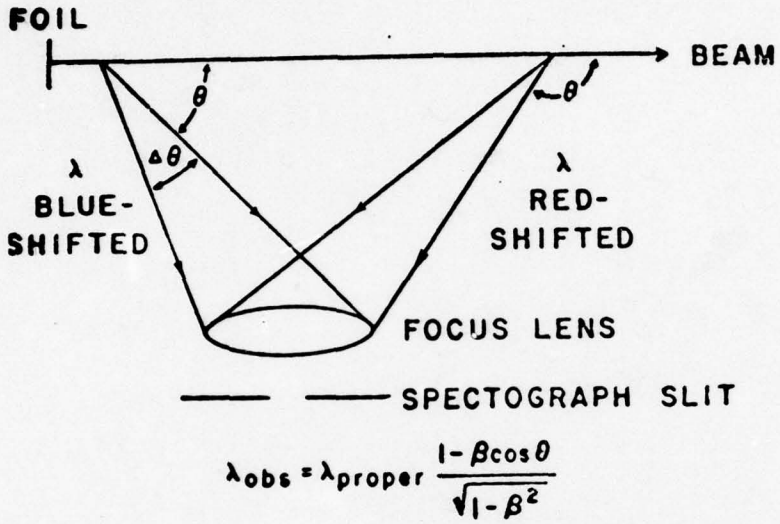

$$\lambda_{obs} = \lambda_{proper} \frac{1-\beta\cos\theta}{\sqrt{1-\beta^2}}$$

Fig. 5

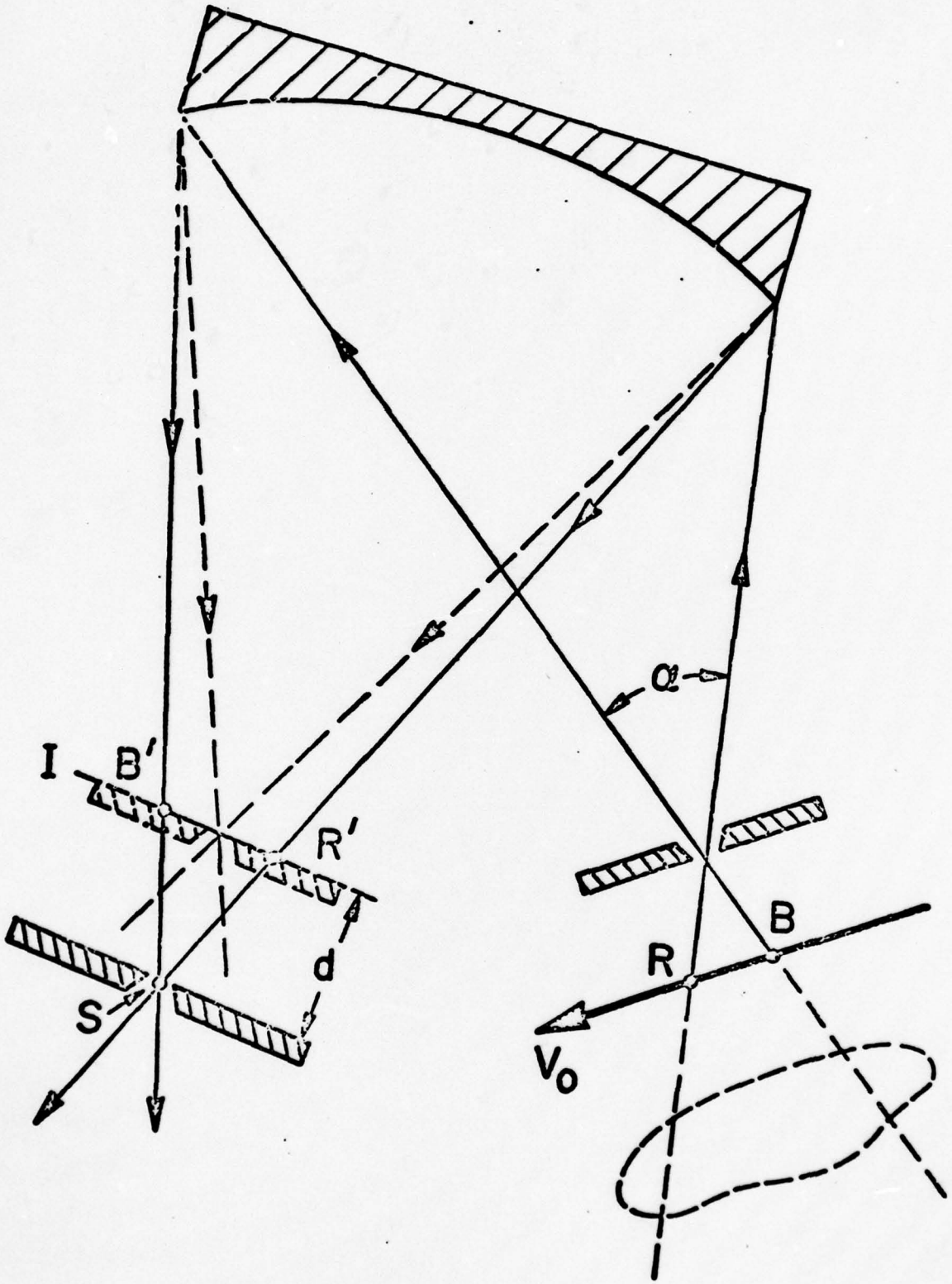

Fig. 6

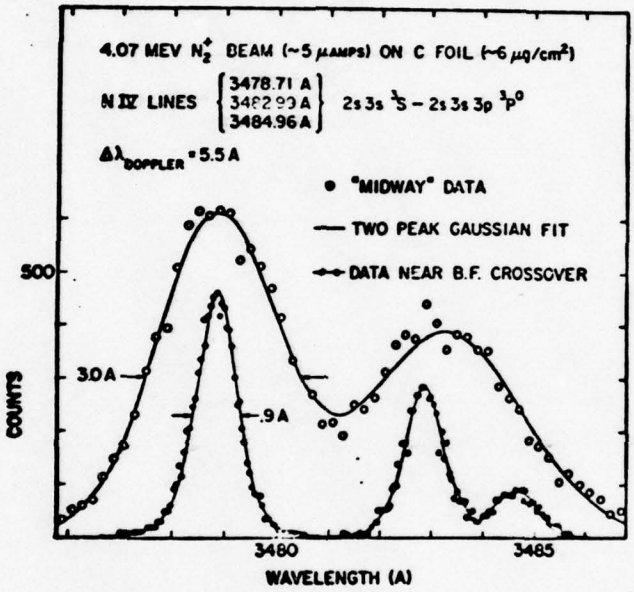
4.07 MEV N_2^+ BEAM (~5 μAMPS) ON C FOIL (~6 μg/cm²)
N IV LINES 3478.71 A, 3482.99 A, 3484.96 A
2s 3s ¹S – 2s 3s 3p ¹P°
$\Delta\lambda_{DOPPLER}$ = 5.5 A
● "MIDWAY" DATA
— TWO PEAK GAUSSIAN FIT
—•— DATA NEAR B.F. CROSSOVER
500
3.0 A
.9 A
COUNTS
3480
3485
WAVELENGTH (A)

Fig. 7

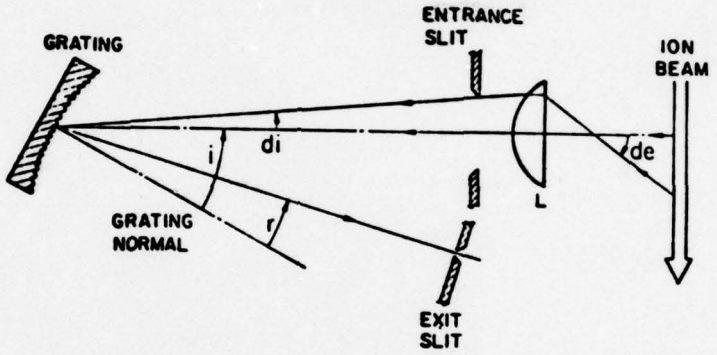
GRATING
ENTRANCE SLIT
ION BEAM
di
i
de
L
GRATING NORMAL
r
EXIT SLIT

Fig. 8

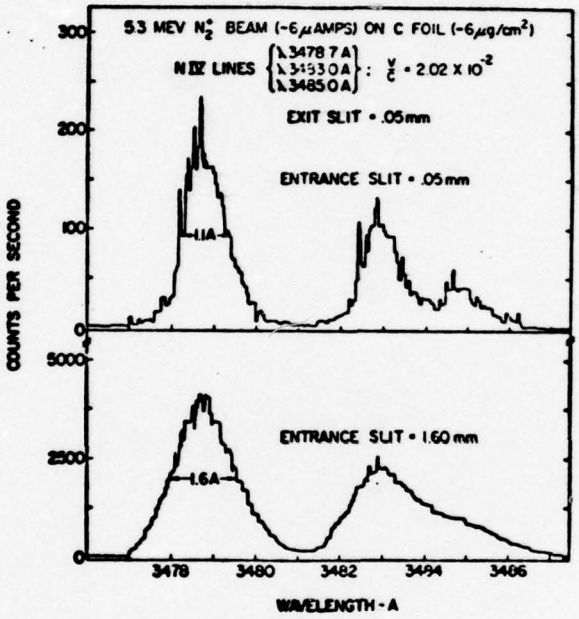
53 MEV N_2^+ BEAM (~6 μAMPS) ON C FOIL (~6 μg/cm²)
N III LINES {λ3478.7 A, λ3483.0 A, λ3485.0 A} : v/c = 2.02 X 10⁻²
EXIT SLIT = .05 mm
ENTRANCE SLIT = .05 mm
1.1A
ENTRANCE SLIT = 1.60 mm
1.6A
COUNTS PER SECOND
300
200
100
0
5000
2500
0
3478
3480
3482
3494
3486
WAVELENGTH - A

Fig. 9

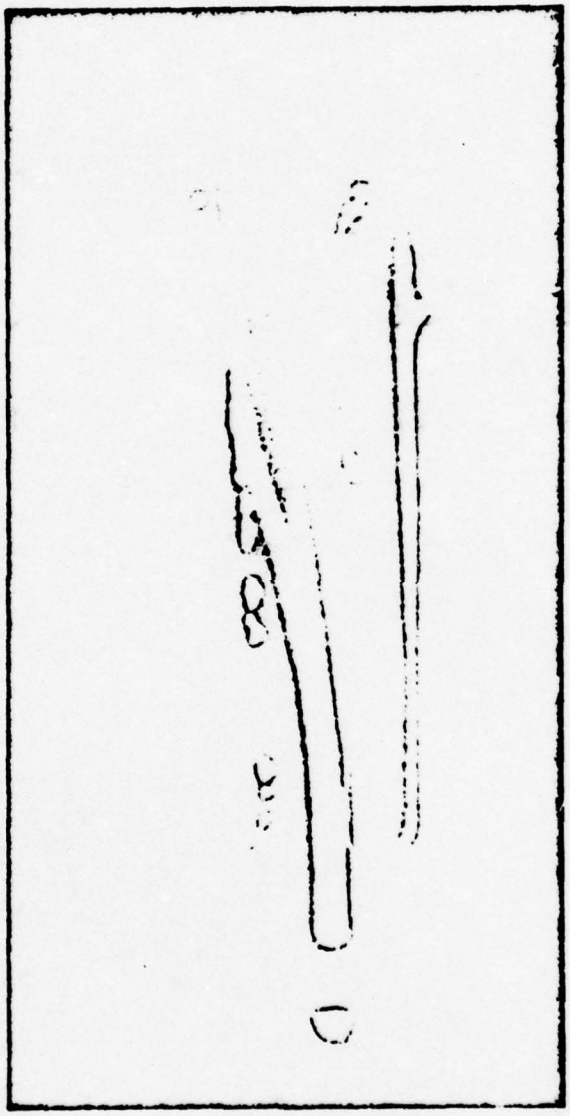

Fig. 10

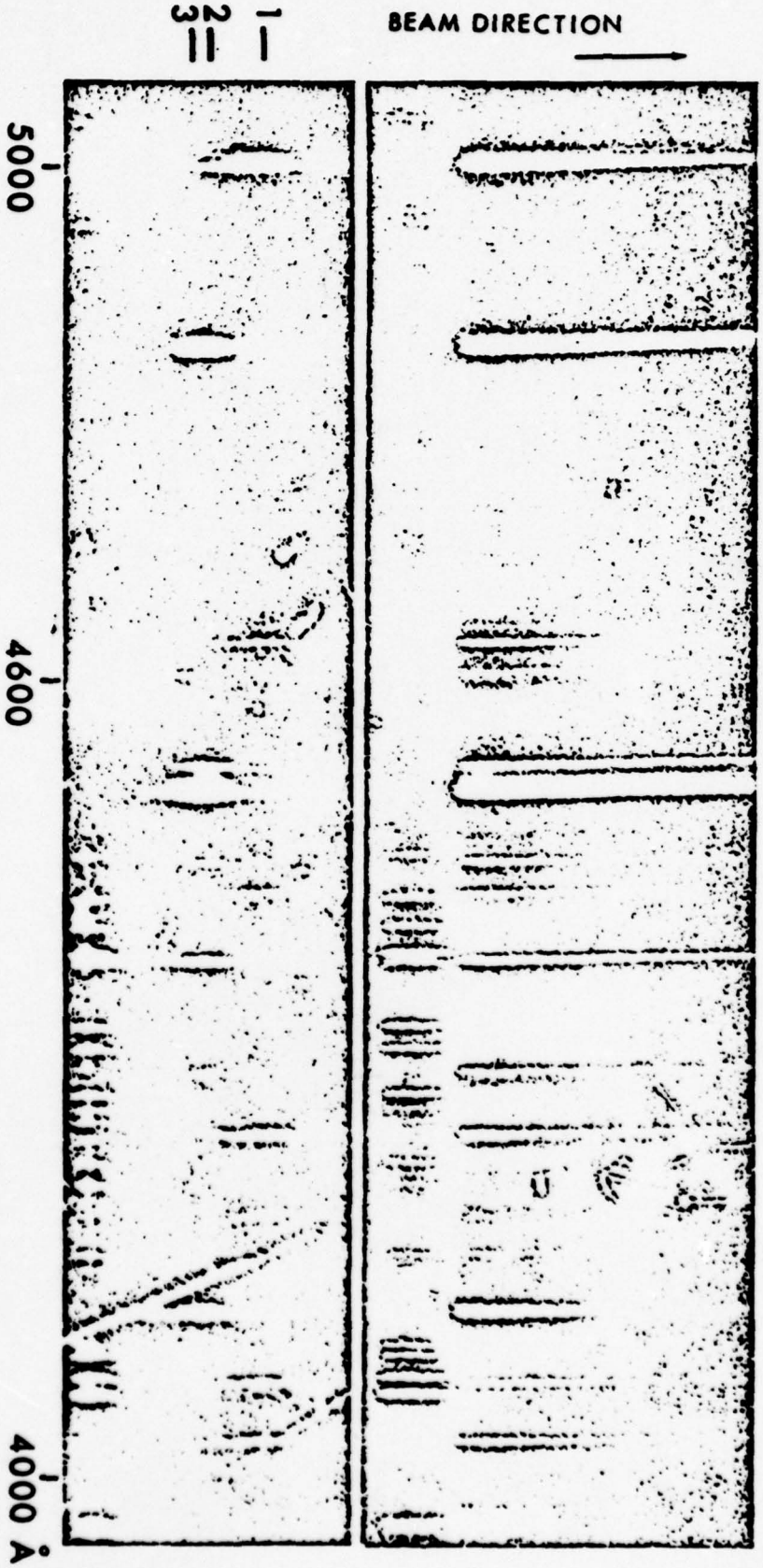

Fig. 11

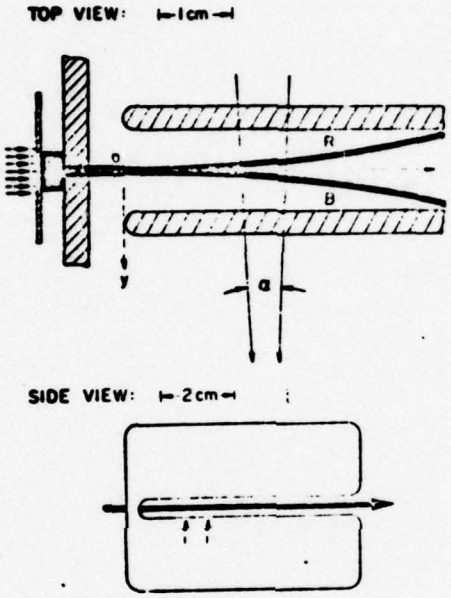

Fig. 12

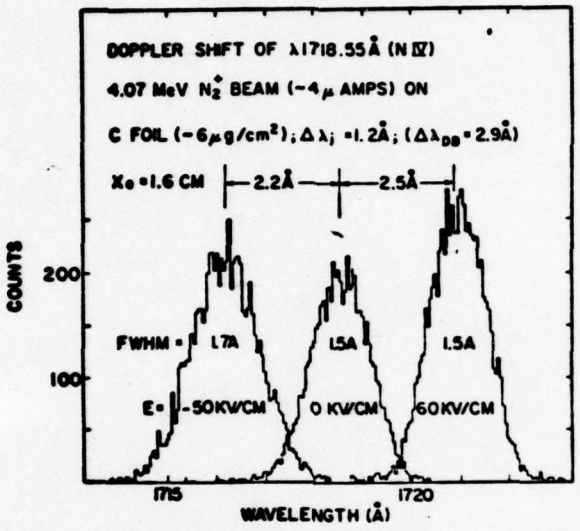
DOPPLER SHIFT OF λ1718.55Å (N IV)
4.07 MeV N_2^+ BEAM (~4μ AMPS) ON
C FOIL (~6μg/cm²); Δλ_i = 1.2Å; (Δλ_DB = 2.9Å)
X_o = 1.6 CM
2.2Å
2.5Å
COUNTS
200
100
FWHM =
1.7Å
1.5Å
1.5Å
E = -50KV/CM
0 KV/CM
60KV/CM
1715
1720
WAVELENGTH (Å)

Fig. 13

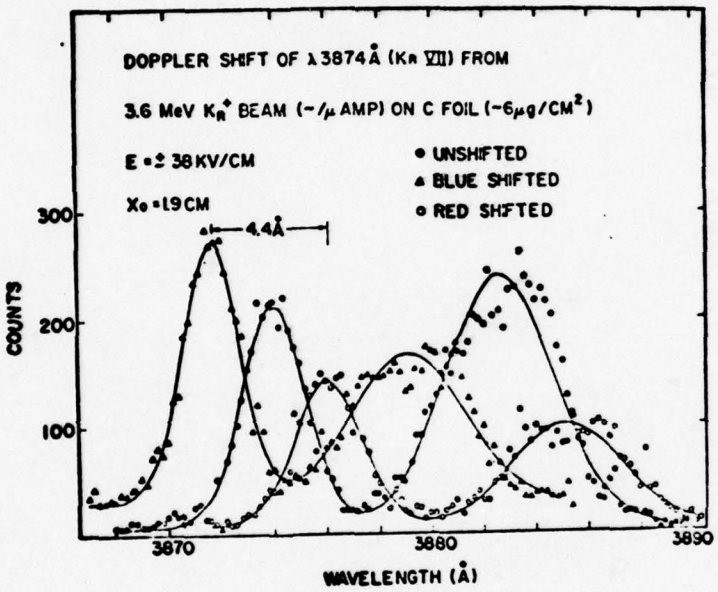
DOPPLER SHIFT OF λ3874Å (Kr VII) FROM
3.6 MeV K_R^+ BEAM (~1μ AMP) ON C FOIL (~6μg/CM²)
E = ± 38 KV/CM
Xo = 1.9 CM
● UNSHIFTED
▲ BLUE SHIFTED
○ RED SHIFTED
4.4Å
COUNTS
300
200
100
3870
3880
3890
WAVELENGTH (Å)

Fig. 14

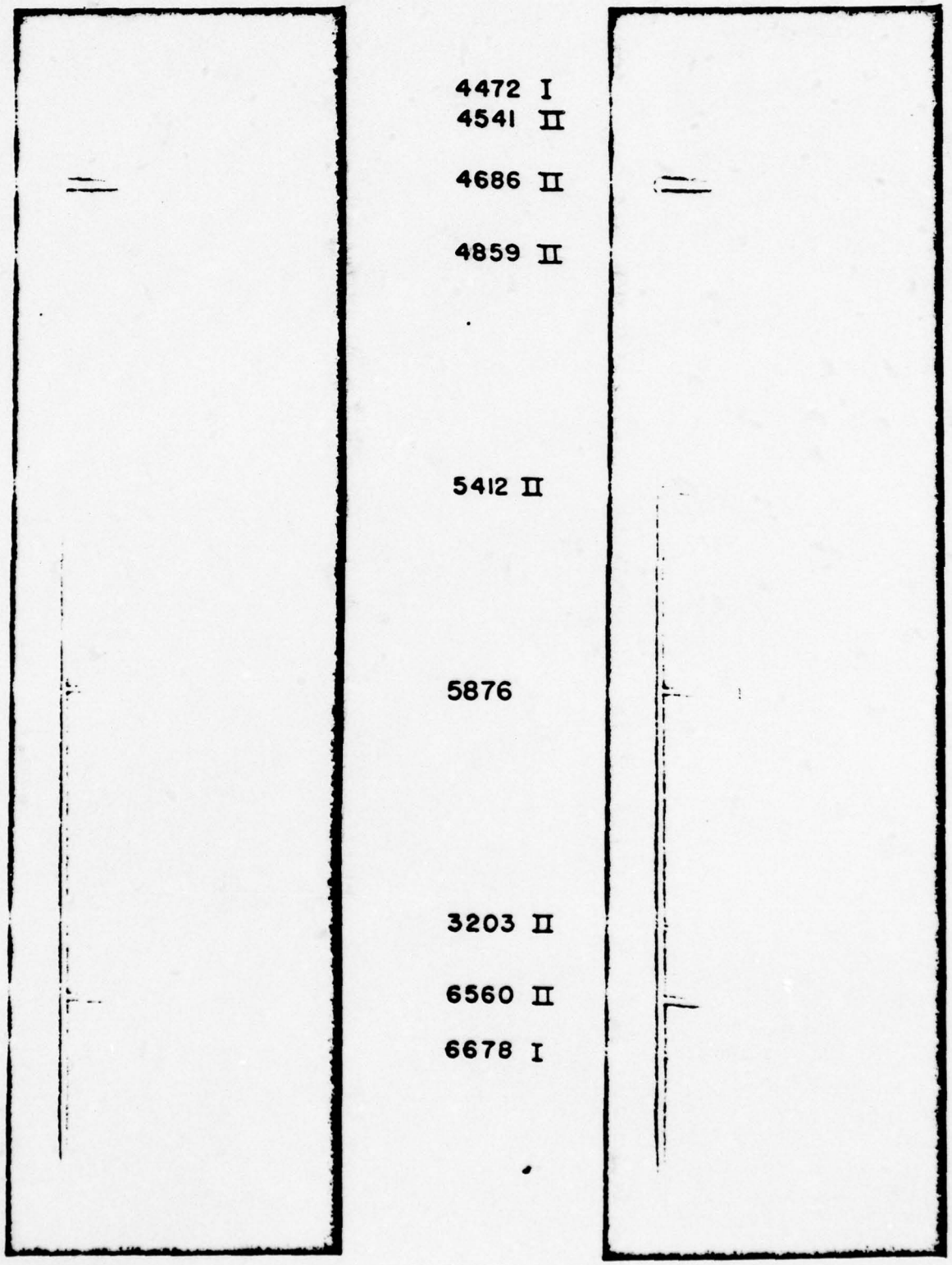
4472 I
4541 II
4686 II
4859 II
5412 II
5876
3203 II
6560 II
6678 I
4472 I
4541 II
4686 II
4859 II
5412 II
5876
3203 II
6560 II
6678 I

Fig. 15

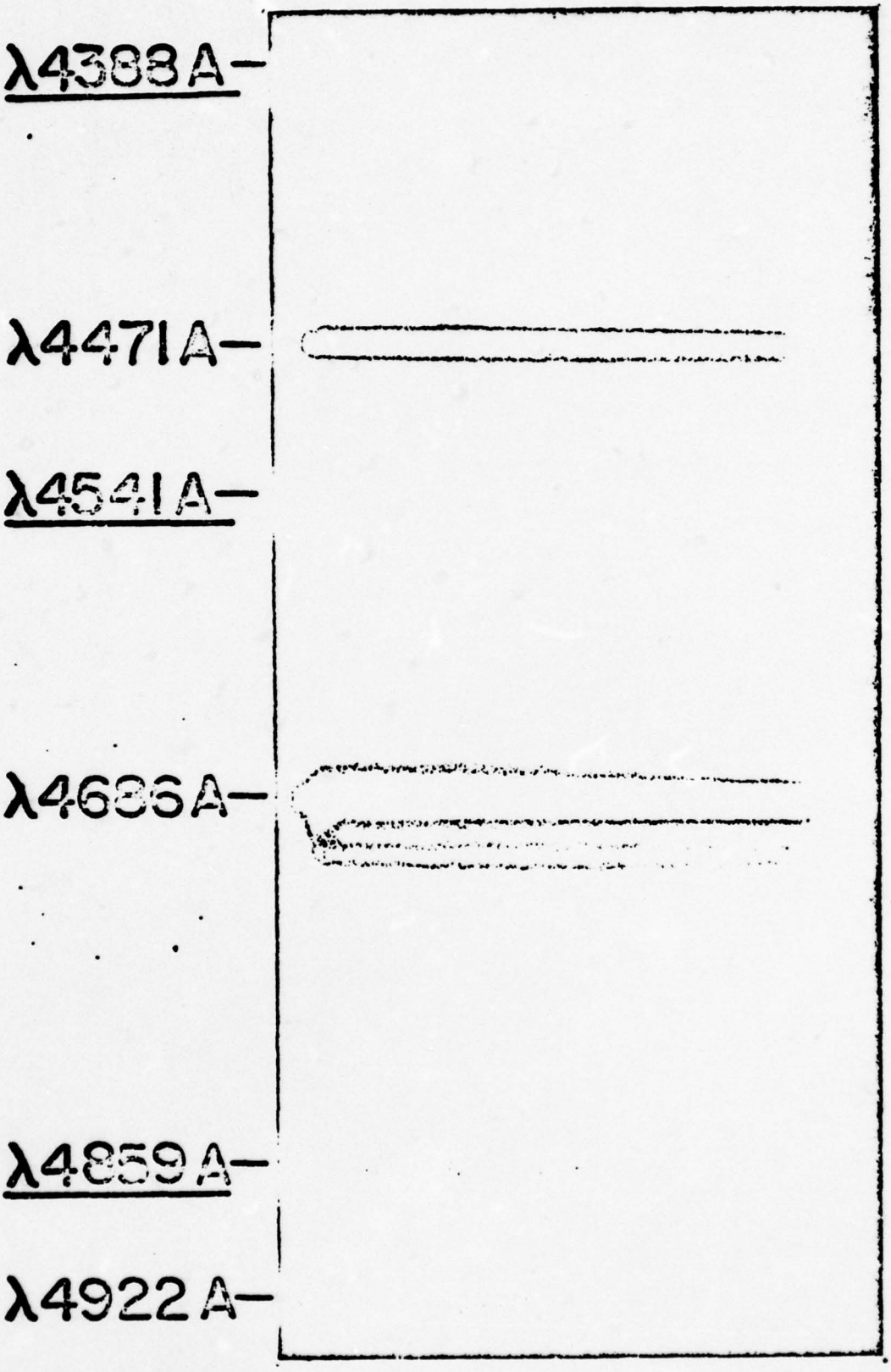

Fig. 16

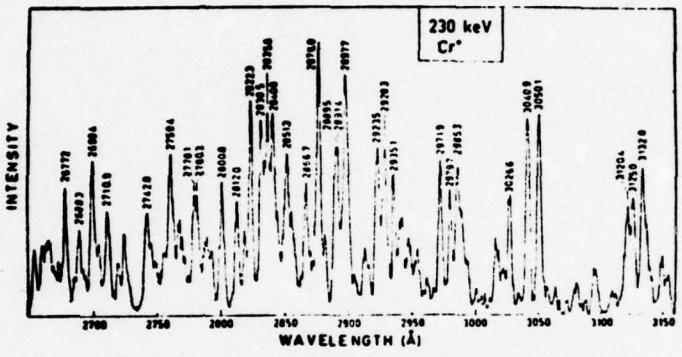

Fig. 17

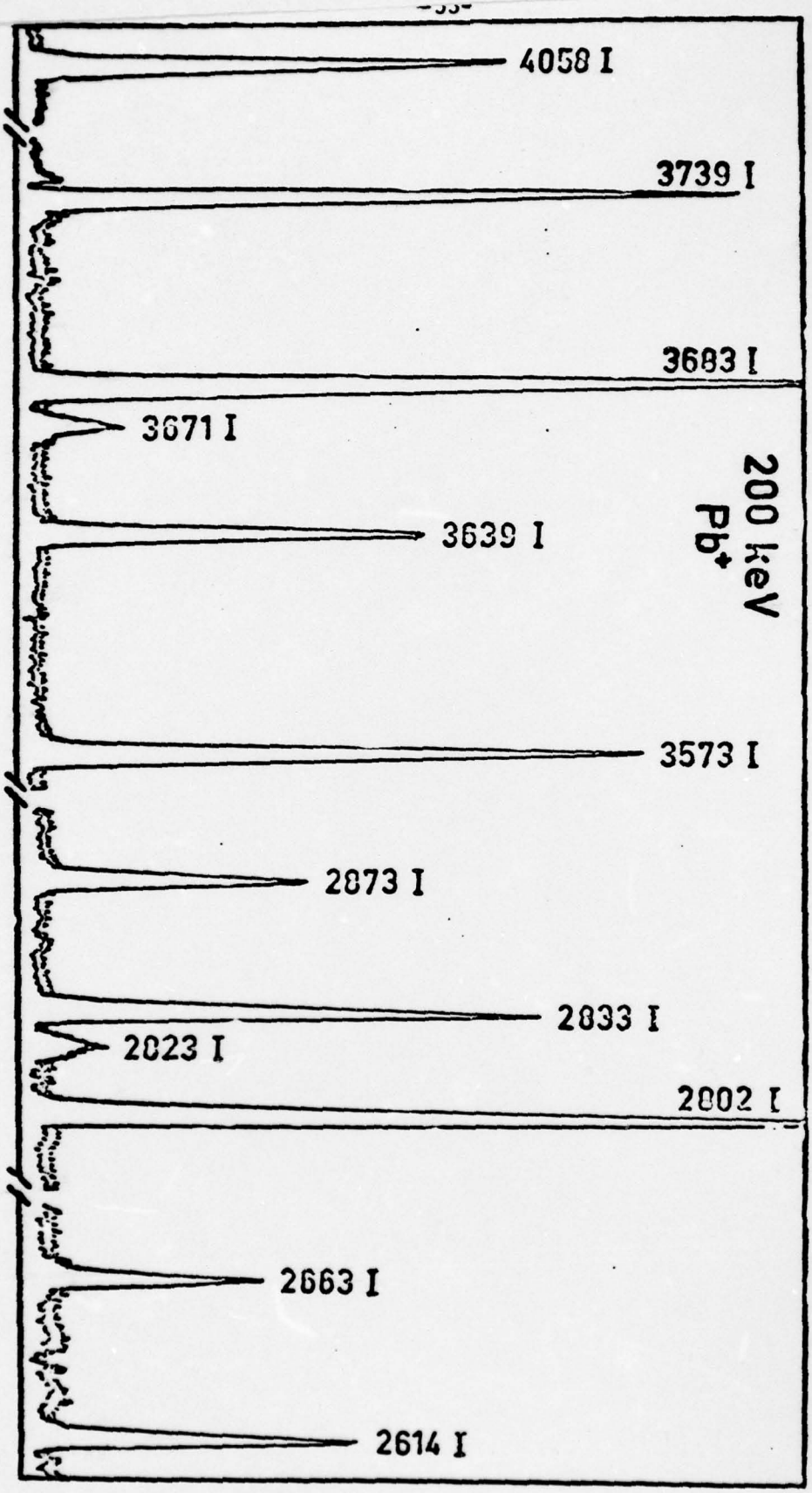
4058 I
3739 I
3683 I
3671 I
3639 I
200 keV
Pb+
3573 I
2873 I
2833 I
2023 I
2802 I
2663 I
2614 I

Fig. 18

Fig. 19

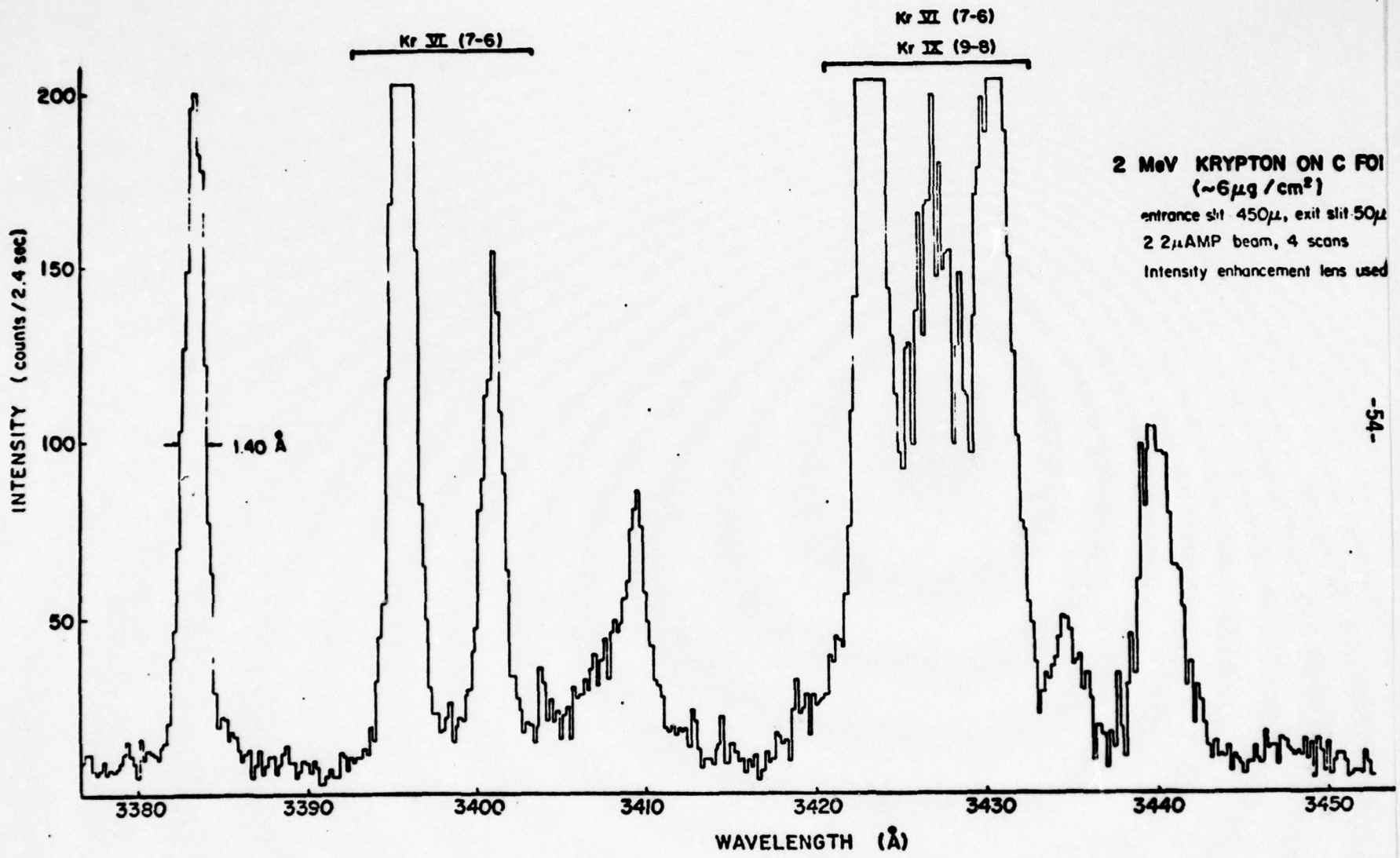
Kr VII (7-6)
Kr VII (7-6)
Kr IX (9-8)
2 MeV KRYPTON ON C FOI
(~6μg/cm²)
entrance slit 450μ, exit slit 50μ
2 2μAMP beam, 4 scans
Intensity enhancement lens used
1.40 Å
INTENSITY (counts/2.4 sec)
200
150
100
50
3380
3390
3400
3410
3420
3430
3440
3450
WAVELENGTH (Å)

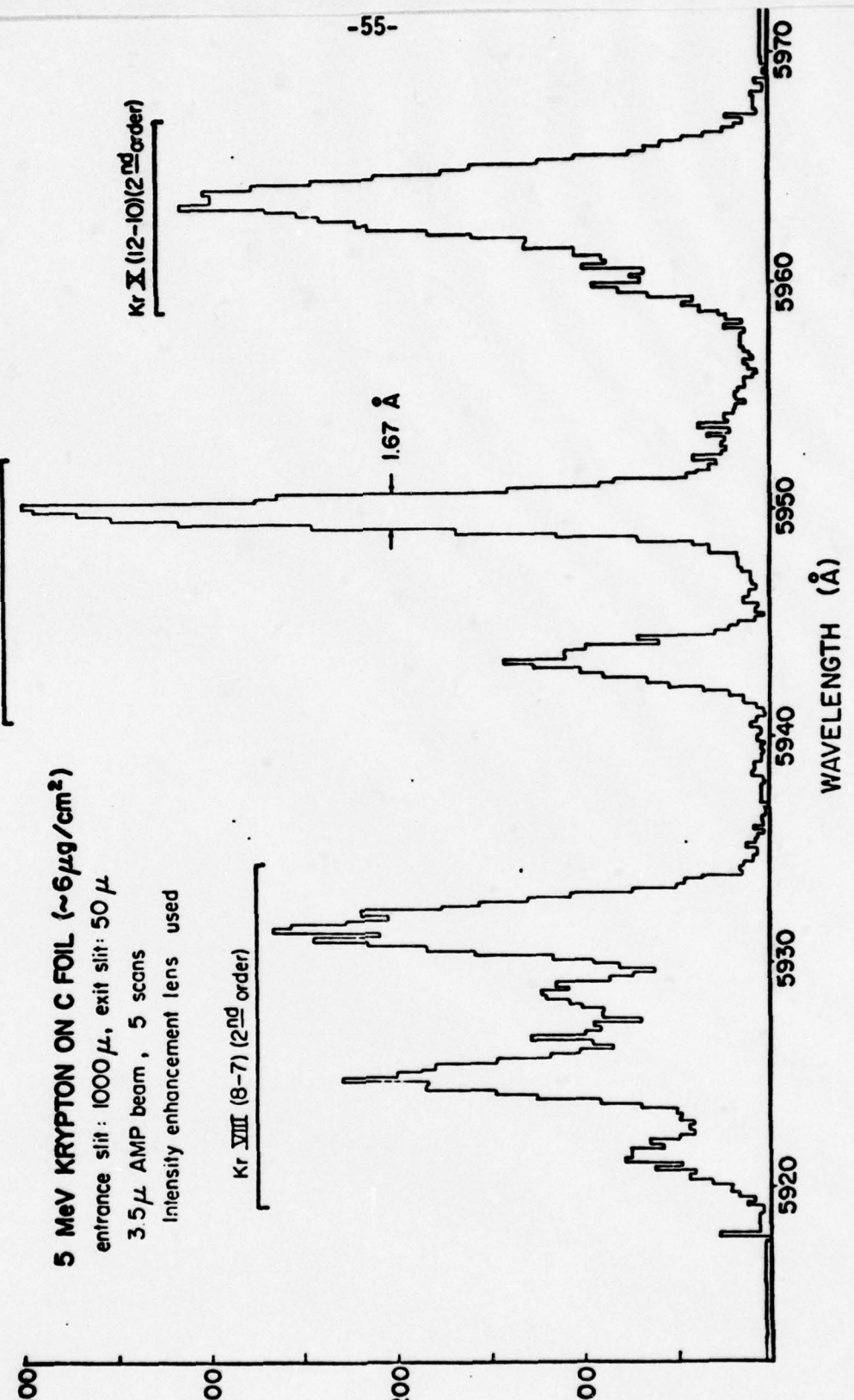
5 MeV KRYPTON ON C FOIL (~6μg/cm²)
entrance slit: 1000μ, exit slit: 50μ
3.5μ AMP beam, 5 scans
Intensity enhancement lens used
Kr VIII (8-7)(2nd order)
Kr VIII (8-7) (2nd order)
Kr X (12-10)(2nd order)
1.67 Å
INTENSITY (counts / 3.0 sec)
WAVELENGTH (Å)
100
200
300
400
5920
5930
5940
5950
5960
5970

Fig. 20

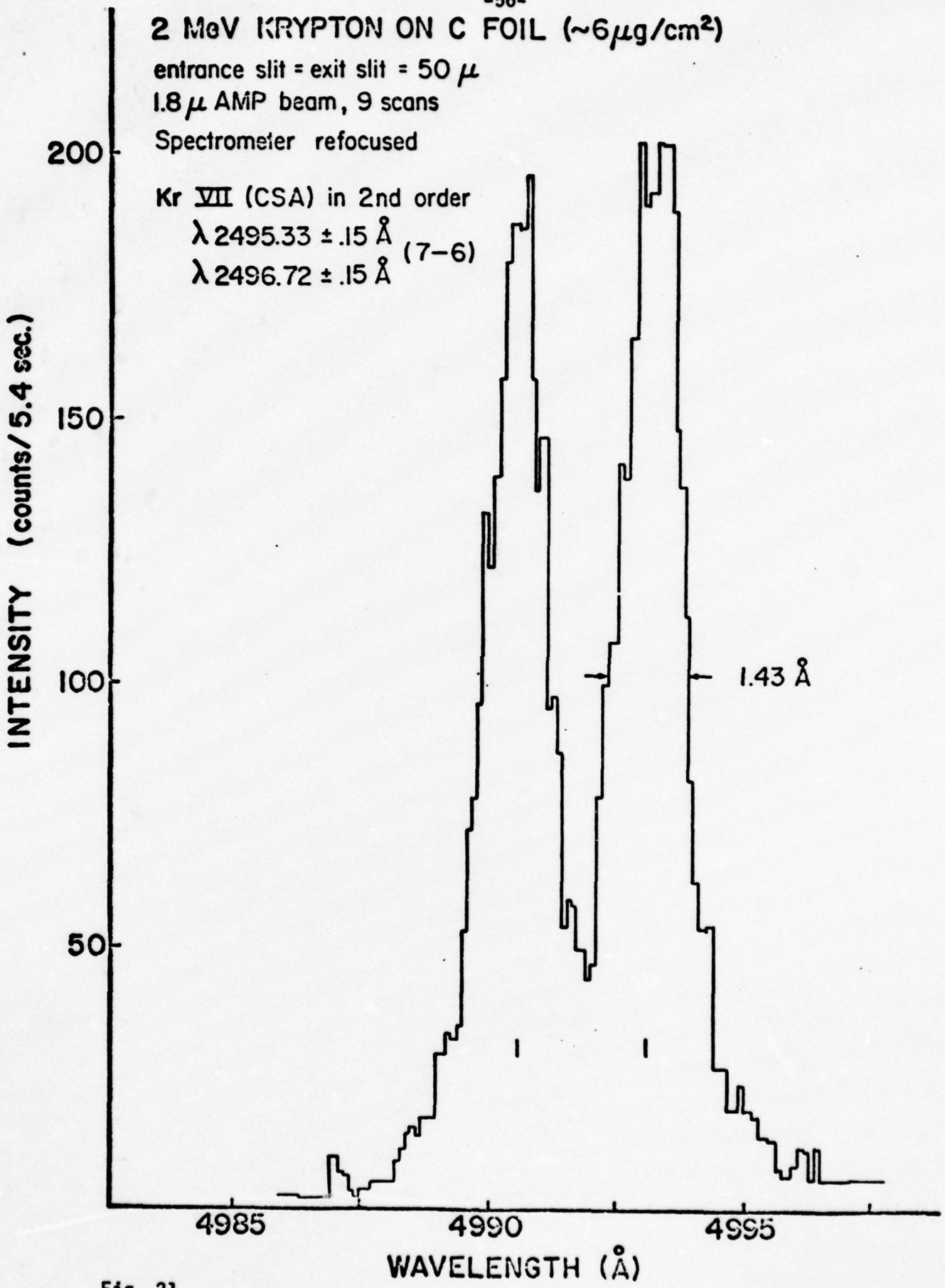
2 MeV KRYPTON ON C FOIL (~6μg/cm²)
entrance slit = exit slit = 50 μ
1.8 μ AMP beam, 9 scans
Spectrometer refocused
Kr VII (CSA) in 2nd order
λ 2495.33 ± .15 Å
λ 2496.72 ± .15 Å (7–6)
1.43 Å
INTENSITY (counts/5.4 sec.)
200
150
100
50
4985
4990
4995
WAVELENGTH (Å)

Fig. 21

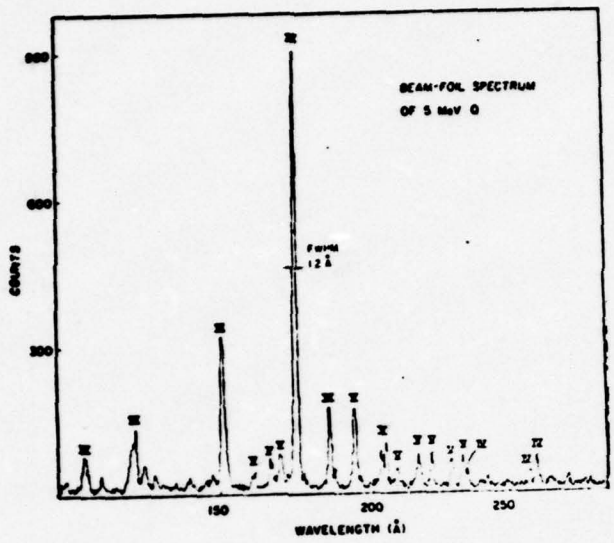
BEAM-FOIL SPECTRUM
OF 5 MeV O
FWHM
1.2 Å
COUNTS
WAVELENGTH (Å)
150
200
250

Fig. 22

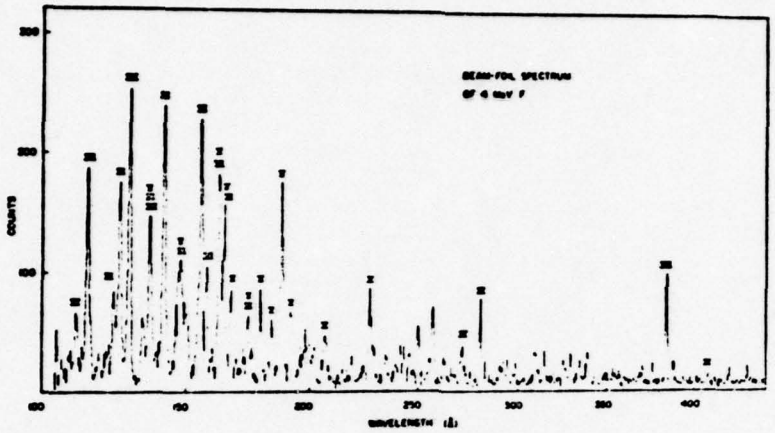

Fig. 23

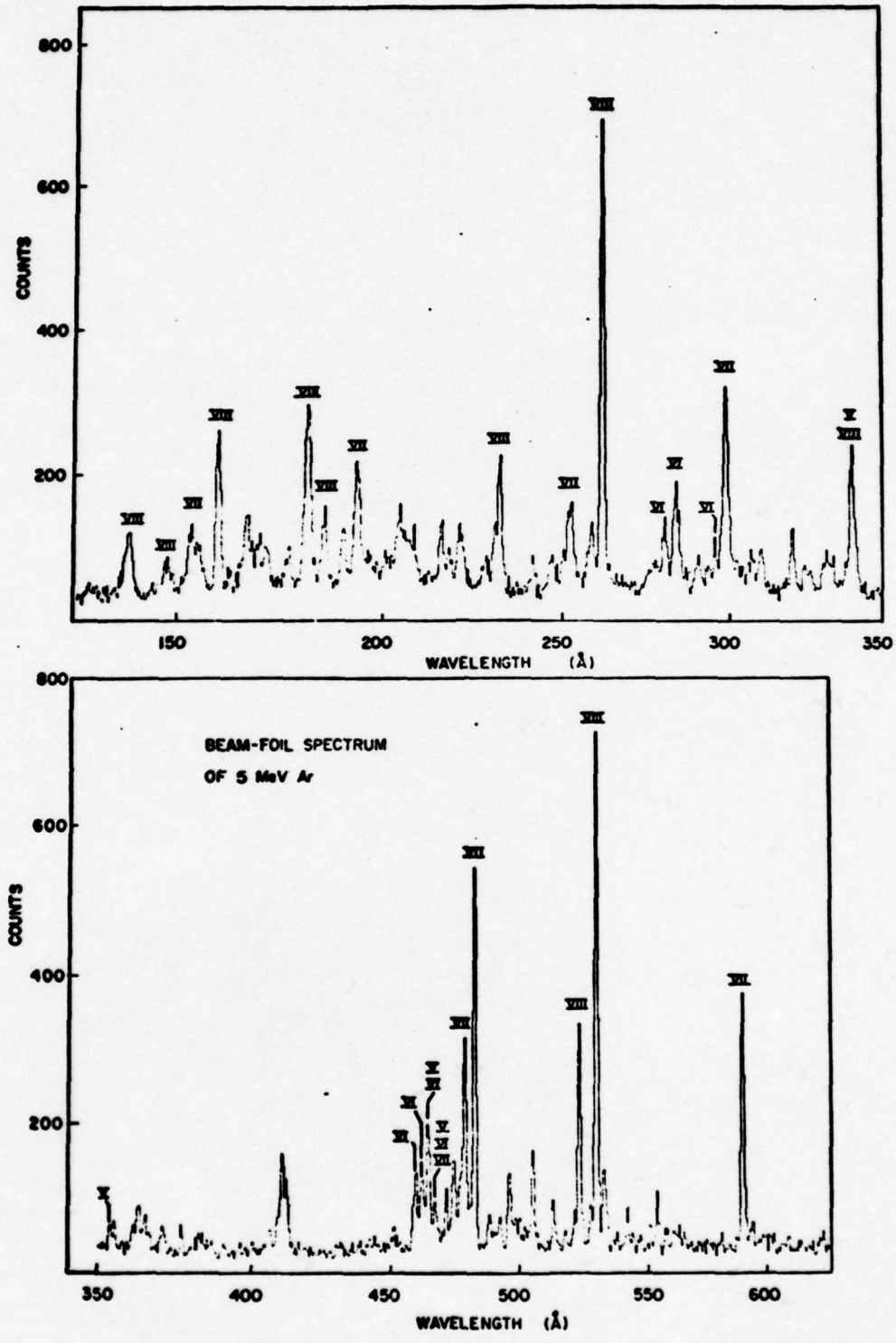
800
600
400
200
COUNTS
150
200
250
300
350
WAVELENGTH (Å)
BEAM-FOIL SPECTRUM
OF 5 MeV Ar
800
600
400
200
COUNTS
350
400
450
500
550
600
WAVELENGTH (Å)

Fig. 24

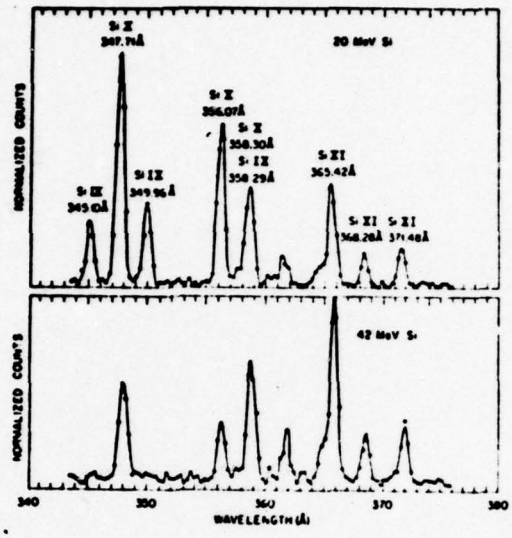
Si X
367.7Å
20 MeV Si
Si X
356.07Å
Si X
358.30Å
Si IX
358.29Å
Si XI
365.42Å
Si IX
349.9Å
Si IX
345.0Å
Si XI
368.28Å
Si XI
371.48Å
NORMALIZED COUNTS
42 MeV Si
340
350
360
370
380
WAVELENGTH (Å)

Fig. 25

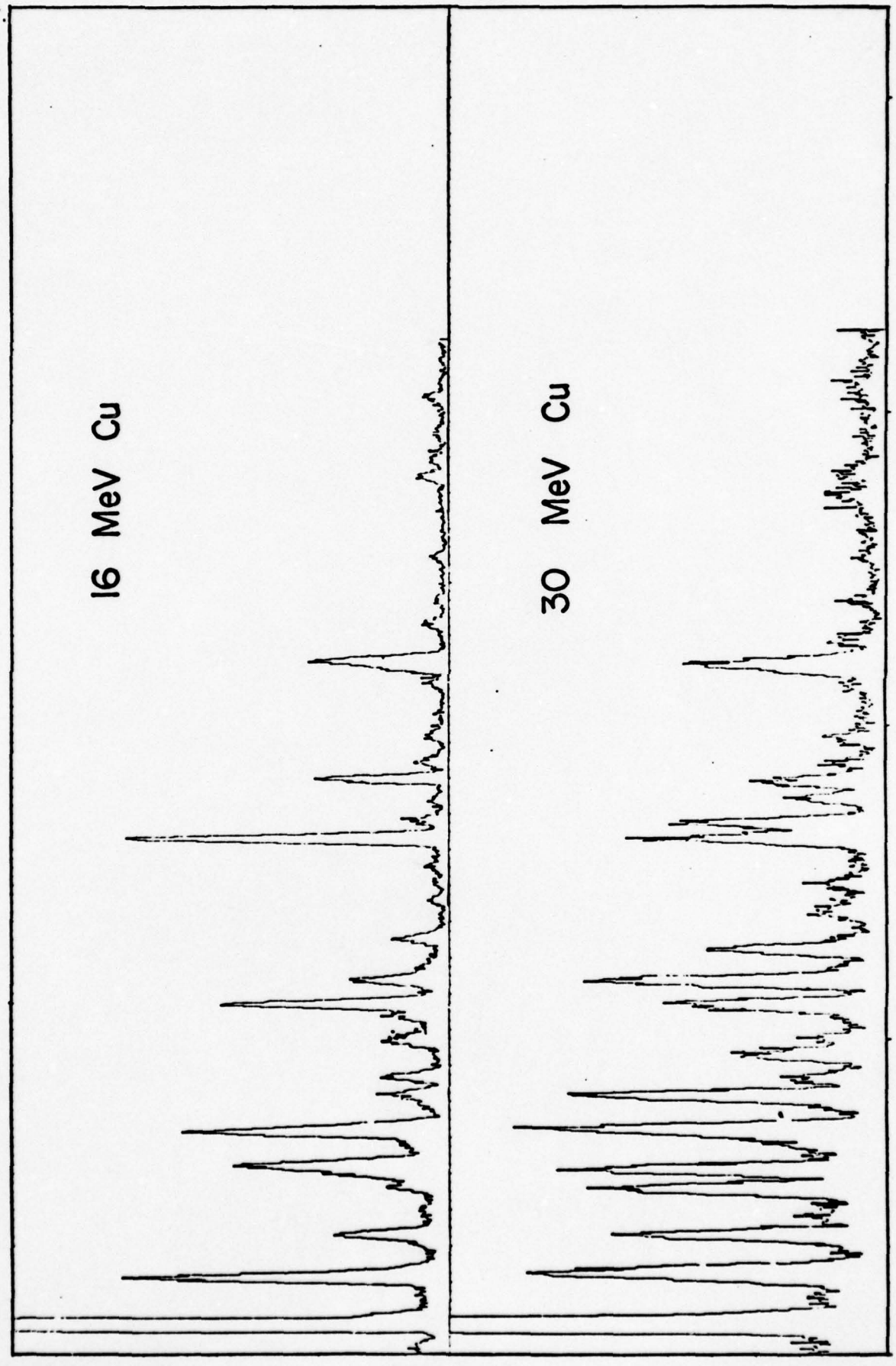
16 MeV Cu
30 MeV Cu
COUNTS
1150
1850
2550
3250
3950
WAVELENGTH (Å)

Fig. 26

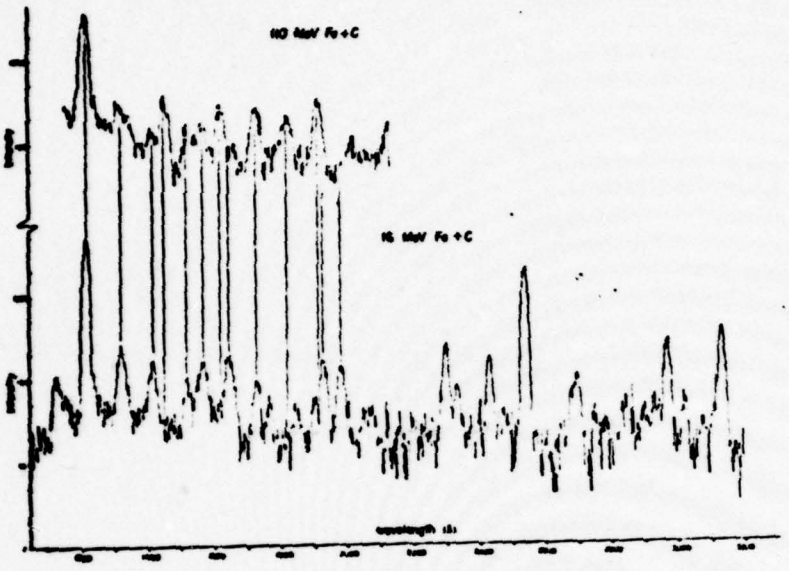

Fig. 27

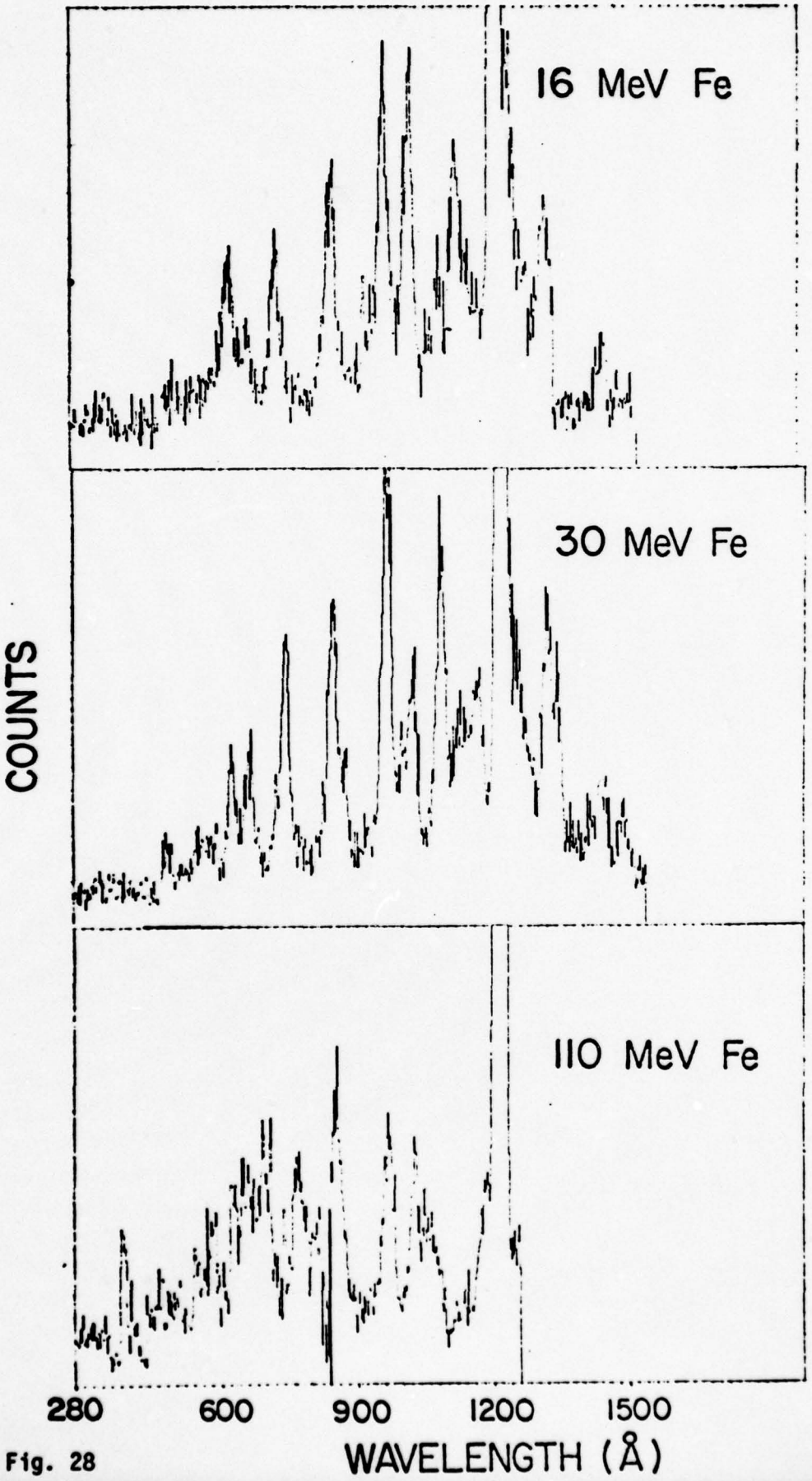
16 MeV Fe
30 MeV Fe
110 MeV Fe
COUNTS
280
600
900
1200
1500
WAVELENGTH (Å)

Fig. 28

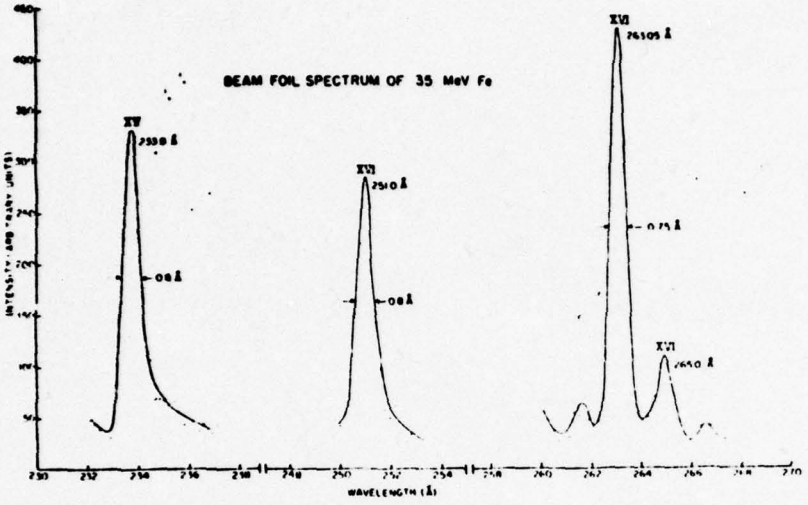
BEAM FOIL SPECTRUM OF 35 MeV Fe
XV
XVI
XVI
WAVELENGTH (Å)

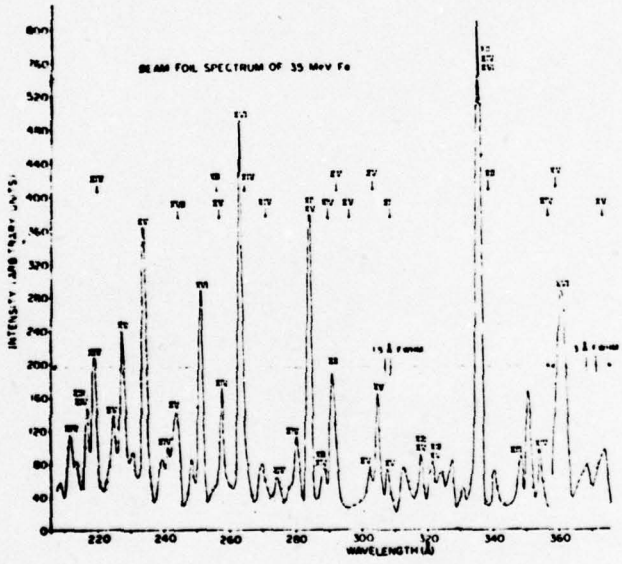
BEAM FOIL SPECTRUM OF 35 MeV Fe
WAVELENGTH (Å)

Fig. 29

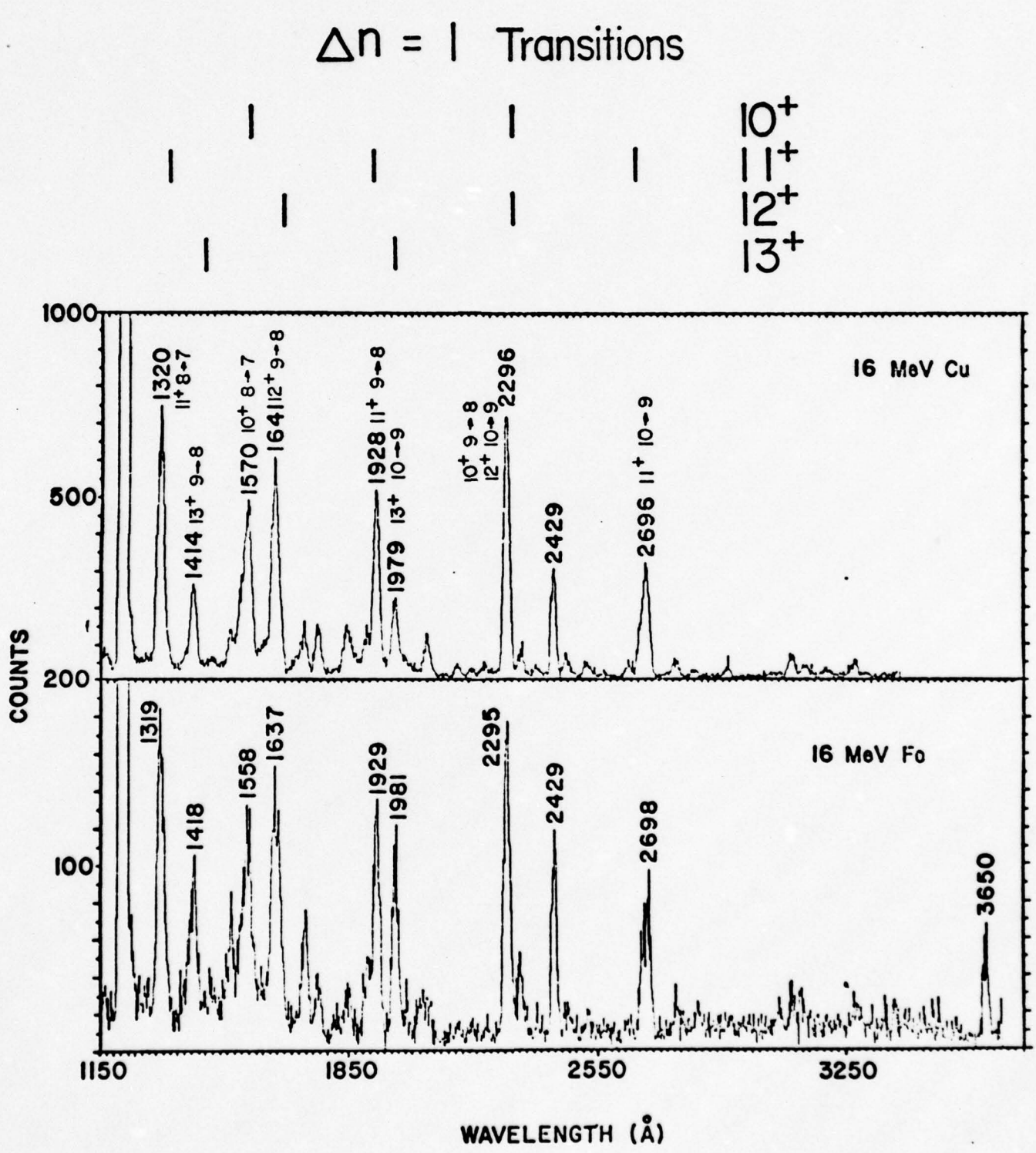
Δn = 1 Transitions
10+
11+
12+
13+
16 MeV Cu
1320
11+ 8→7
1414 13+ 9→8
1570 10+ 8→7
1641 12+ 9→8
1928 11+ 9→8
1979 13+ 10→9
10+ 9→8
12+ 10→9
2296
2429
2696 11+ 10→9
16 MeV Fo
1319
1418
1558
1637
1929
1981
2295
2429
2698
3650
1000
500
200
100
COUNTS
1150
1850
2550
3250
WAVELENGTH (Å)

Fig. 30

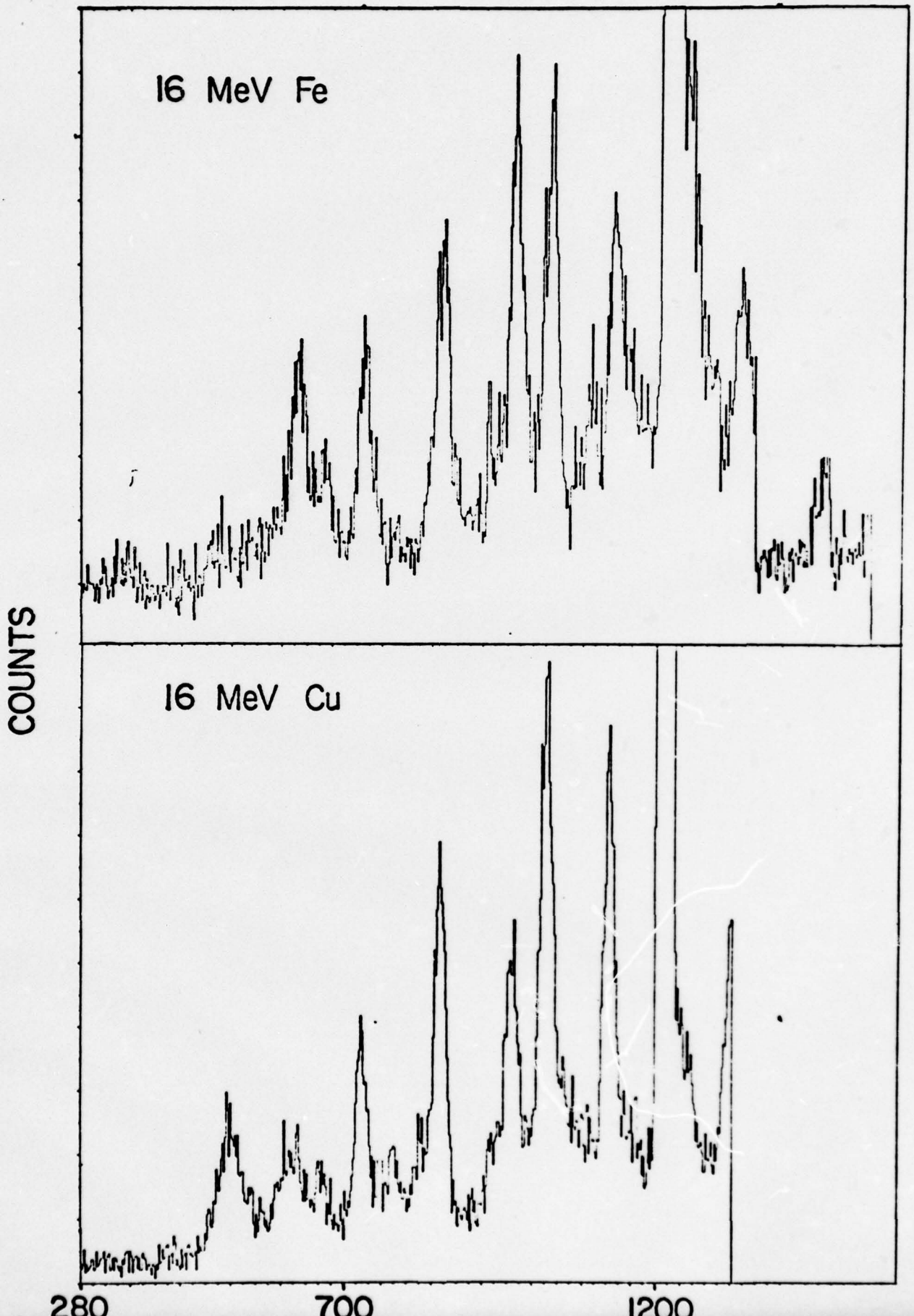
16 MeV Fe
16 MeV Cu
COUNTS
280
700
1200
WAVELENGTH (Å)

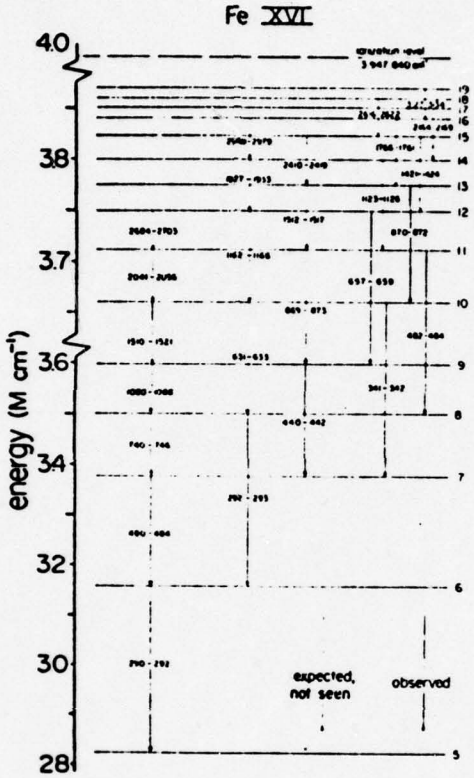
Fe XVI
4.0
3.8
3.7
3.6
3.4
3.2
3.0
2.8
energy (M cm⁻¹)
ionization level
3 947 840 cm⁻¹
19
18
17
16
15
14
13
12
11
10
9
8
7
6
5
expected, not seen
observed

Fig. 32

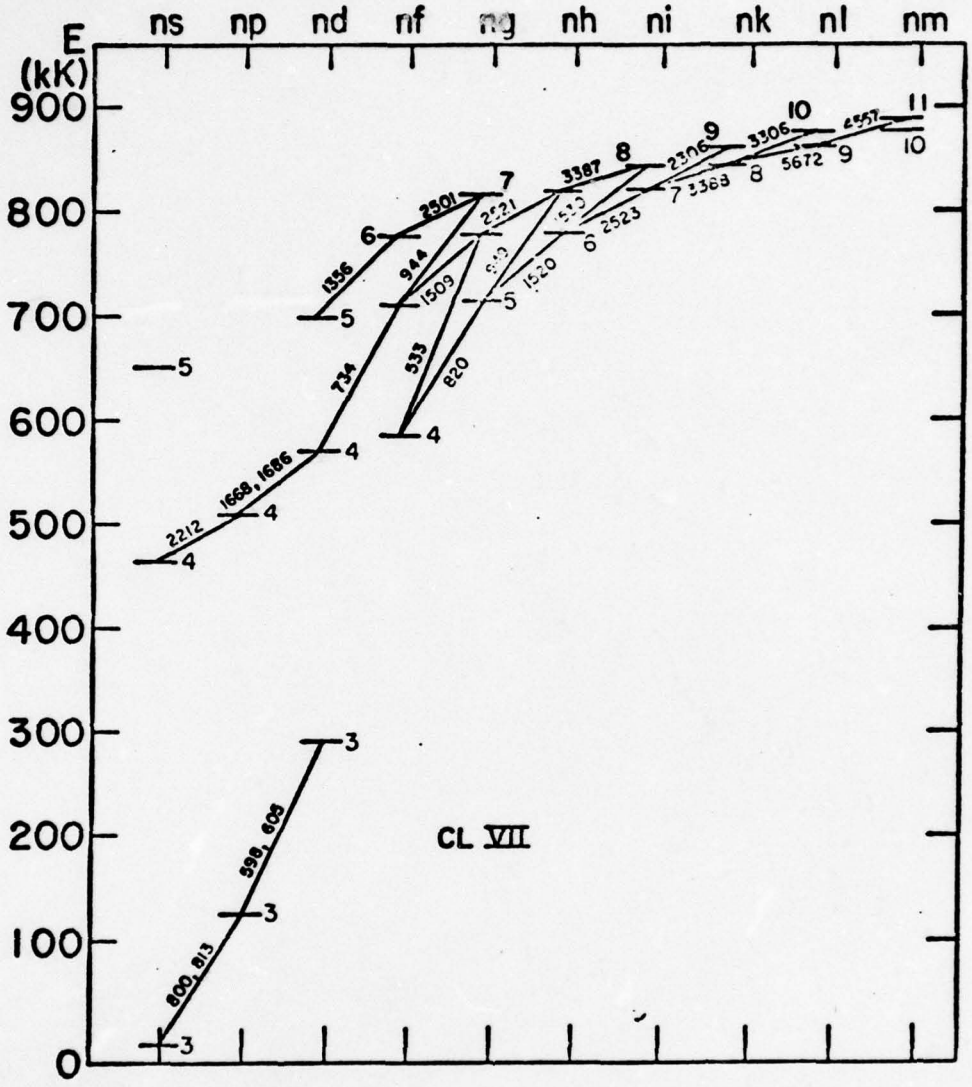
E
(kK)
ns
np
nd
nf
ng
nh
ni
nk
nl
nm
900
800
700
600
500
400
300
200
100
0
CL VII

Fig. 33

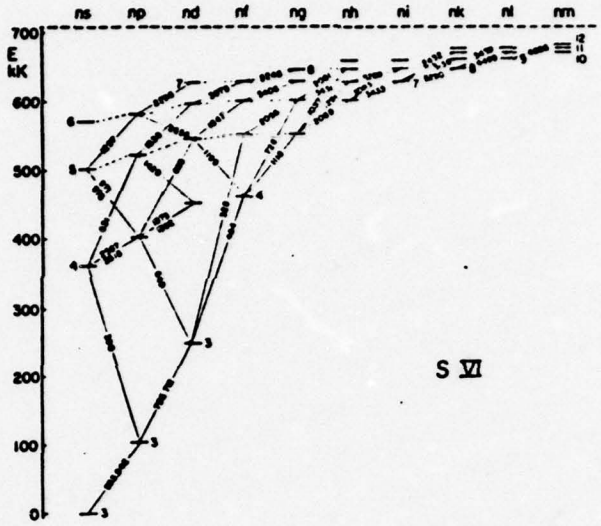

Fig. 34

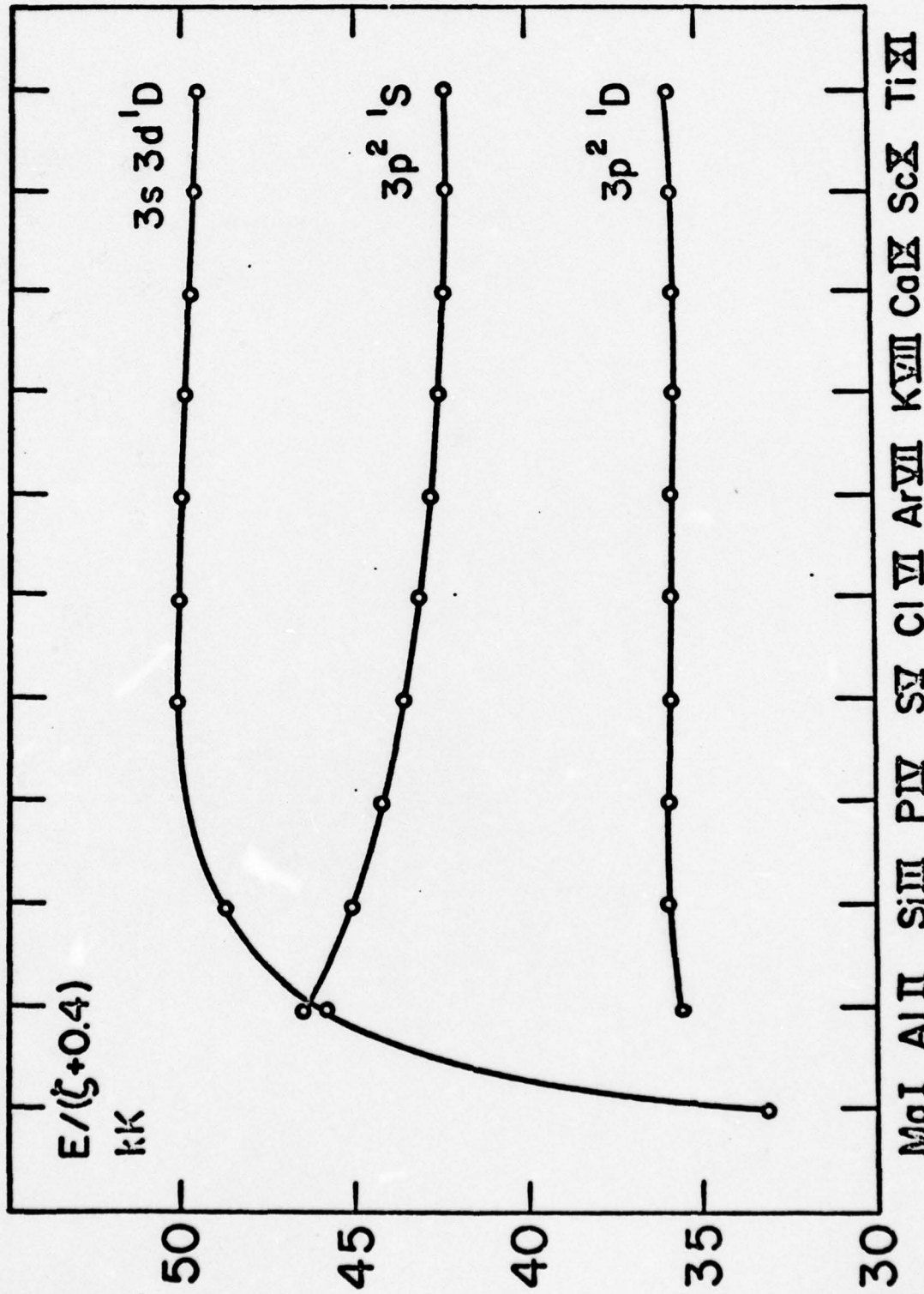
E/(ζ+0.4)
kK
50
45
40
35
30
3s 3d ¹D
3p² ¹S
3p² ¹D
Mg I Al II Si III P IV S V Cl VI Ar VII K VIII Ca IX Sc X Ti XI

Fig. 35

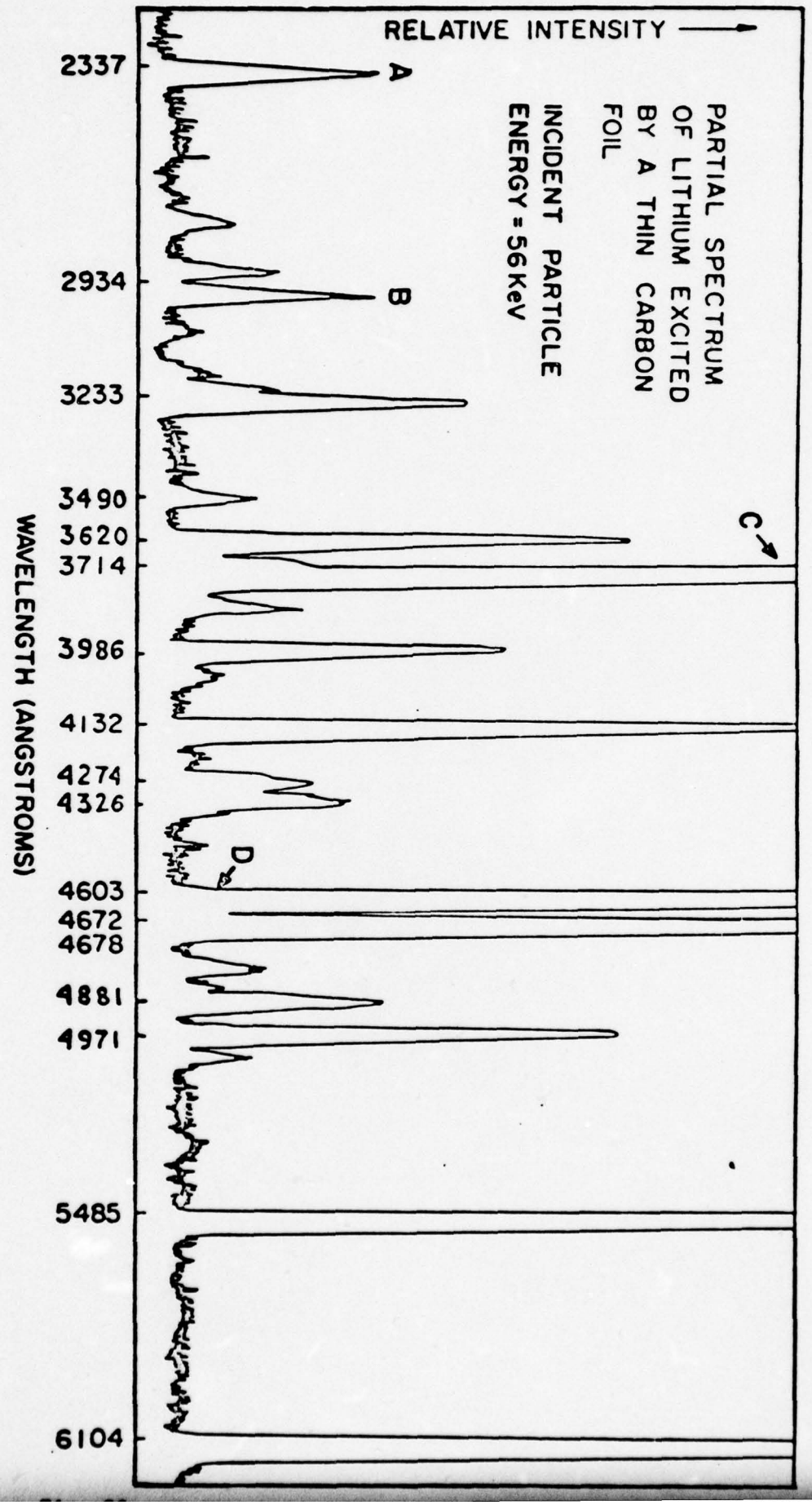
RELATIVE INTENSITY
PARTIAL SPECTRUM OF LITHIUM EXCITED BY A THIN CARBON FOIL
INCIDENT PARTICLE ENERGY = 56 KeV
A
B
C
D
2337
2934
3233
3490
3620
3714
3986
4132
4274
4326
4603
4672
4678
4881
4971
5485
6104
WAVELENGTH (ANGSTROMS)

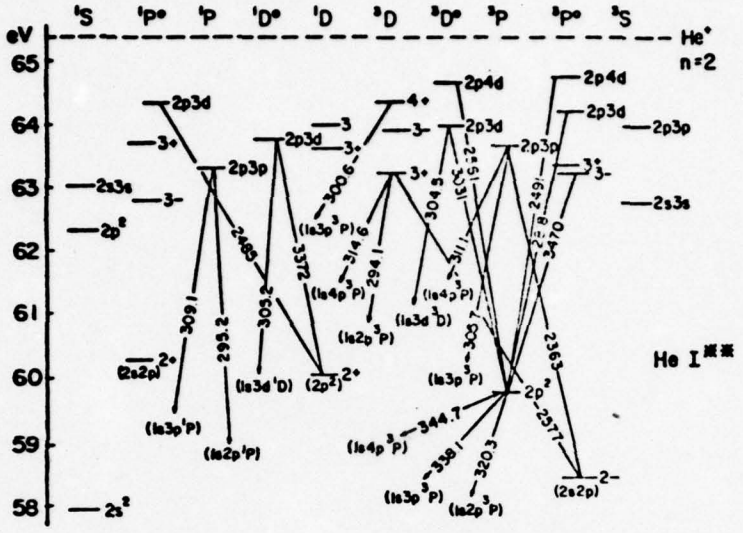
1S
1P°
1P
1D°
1D
3D
3D°
3P
3P°
3S
eV
He+
n=2
65
64
63
62
61
60
59
58
2p3d
3+
2p3p
2s3s
3-
2p²
2+
(2s2p)
(1s3p¹P)
(1s2p¹P)
(1s3d¹D)
(2p²)2+
2p3d
3
3+
3-
4+
2p4d
2p3d
(1s3p³P)
(1s4p³P)
(1s2p³P)
(1s3d³D)
(1s3p³P)
2p²
(1s4p³P)
(1s3p³P)
(1s2p³P)
2p4d
2p3d
2p3p
3+
3-
2s3s
(2s2p)
2-
He I**

Fig. 37

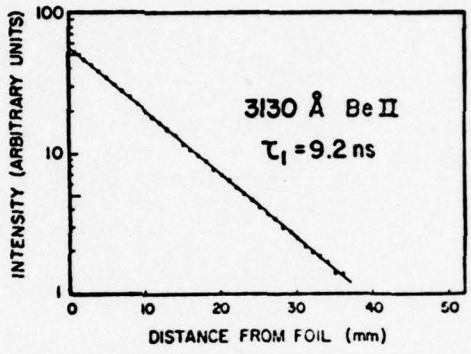
100
10
1
INTENSITY (ARBITRARY UNITS)
3130 Å Be II
τ_1 = 9.2 ns
0
10
20
30
40
50
DISTANCE FROM FOIL (mm)

Fig. 38

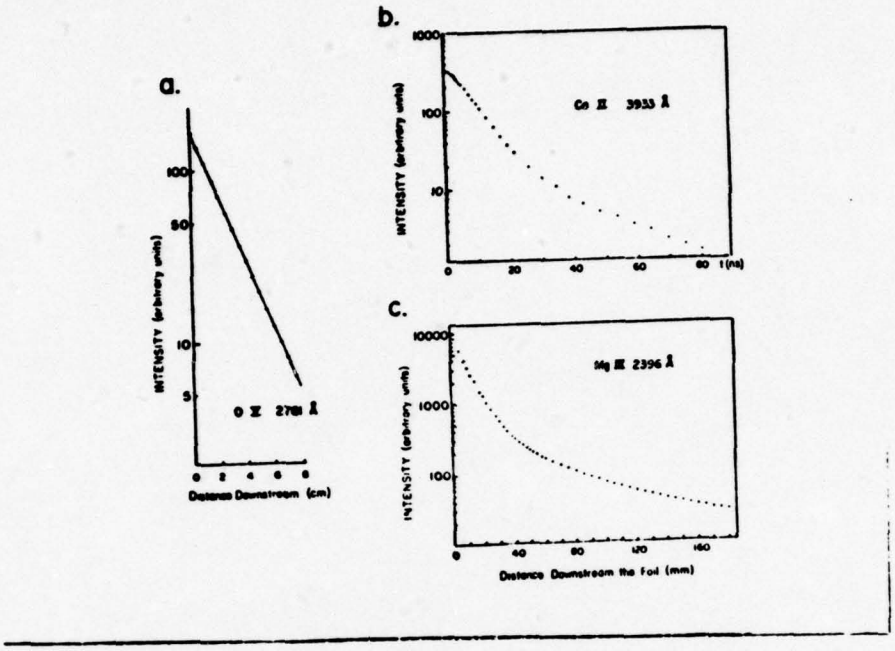
a.
INTENSITY (arbitrary units)
100
50
10
5
O II 2781 Å
0
2
4
6
8
Distance Downstream (cm)
b.
INTENSITY (arbitrary units)
1000
100
10
Co II 3933 Å
0
20
40
60
80
t (ns)
c.
INTENSITY (arbitrary units)
10000
1000
100
Mg II 2396 Å
0
40
80
120
160
Distance Downstream the Foil (mm)

Fig. 39

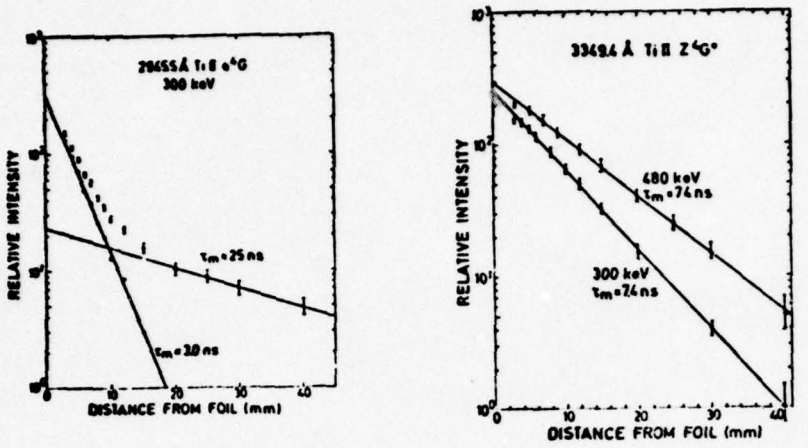
RELATIVE INTENSITY
DISTANCE FROM FOIL (mm)
τm = 25 ns
τm = 2.0 ns
480 keV
τm = 7.4 ns
300 keV
τm = 7.4 ns

Fig. 40

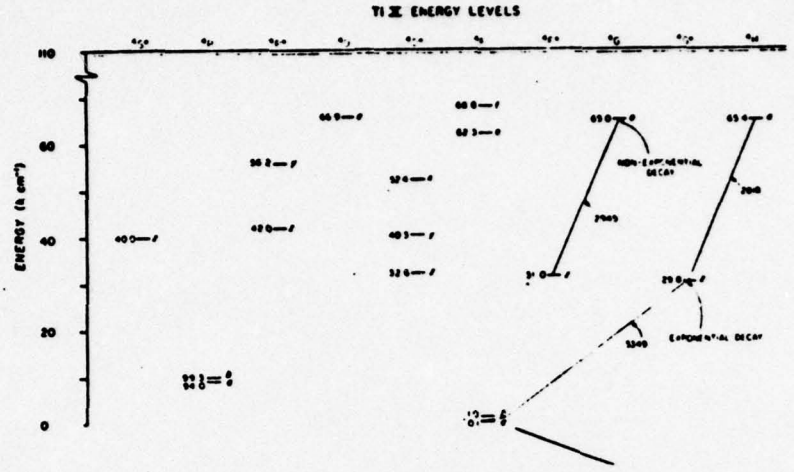
Ti ☒ ENERGY LEVELS
ENERGY (h cm⁻¹)
110
80
40
20
0
EXPONENTIAL DECAY

Fig. 41

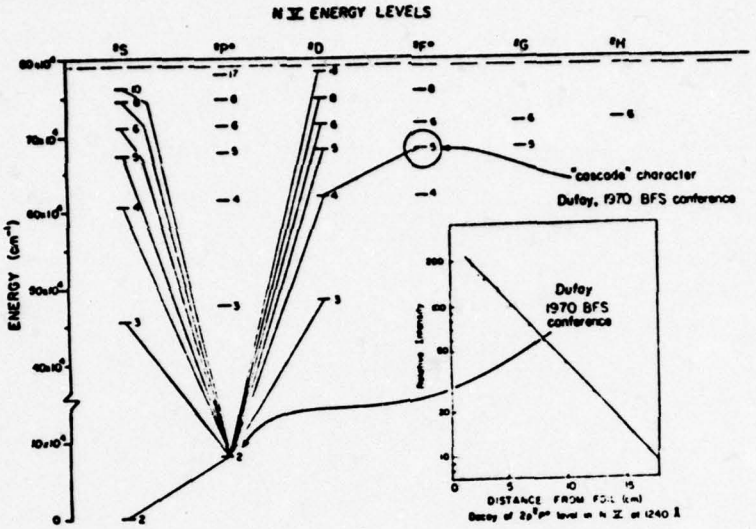
N II ENERGY LEVELS
ENERGY (cm⁻¹)
"cascade" character
Dufay, 1970 BFS conference
Dufay
1970 BFS
conference
DISTANCE FROM FOIL (cm)

Fig. 42

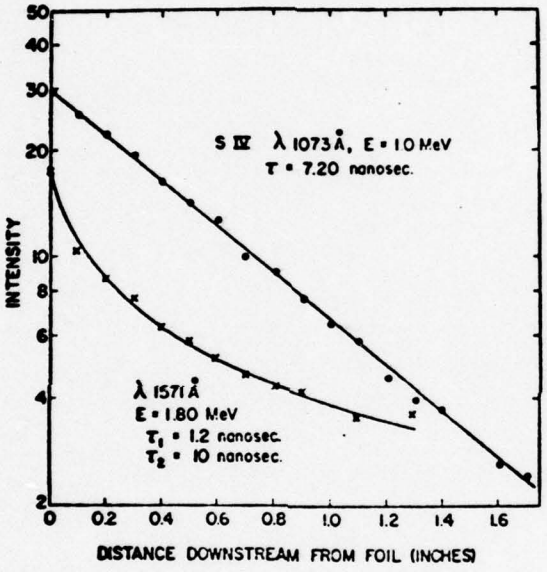
S III λ 1073Å, E = 1.0 MeV
τ = 7.20 nanosec.
λ 1571 Å
E = 1.80 MeV
τ1 = 1.2 nanosec.
τ2 = 10 nanosec.
INTENSITY
DISTANCE DOWNSTREAM FROM FOIL (INCHES)

Fig. 43

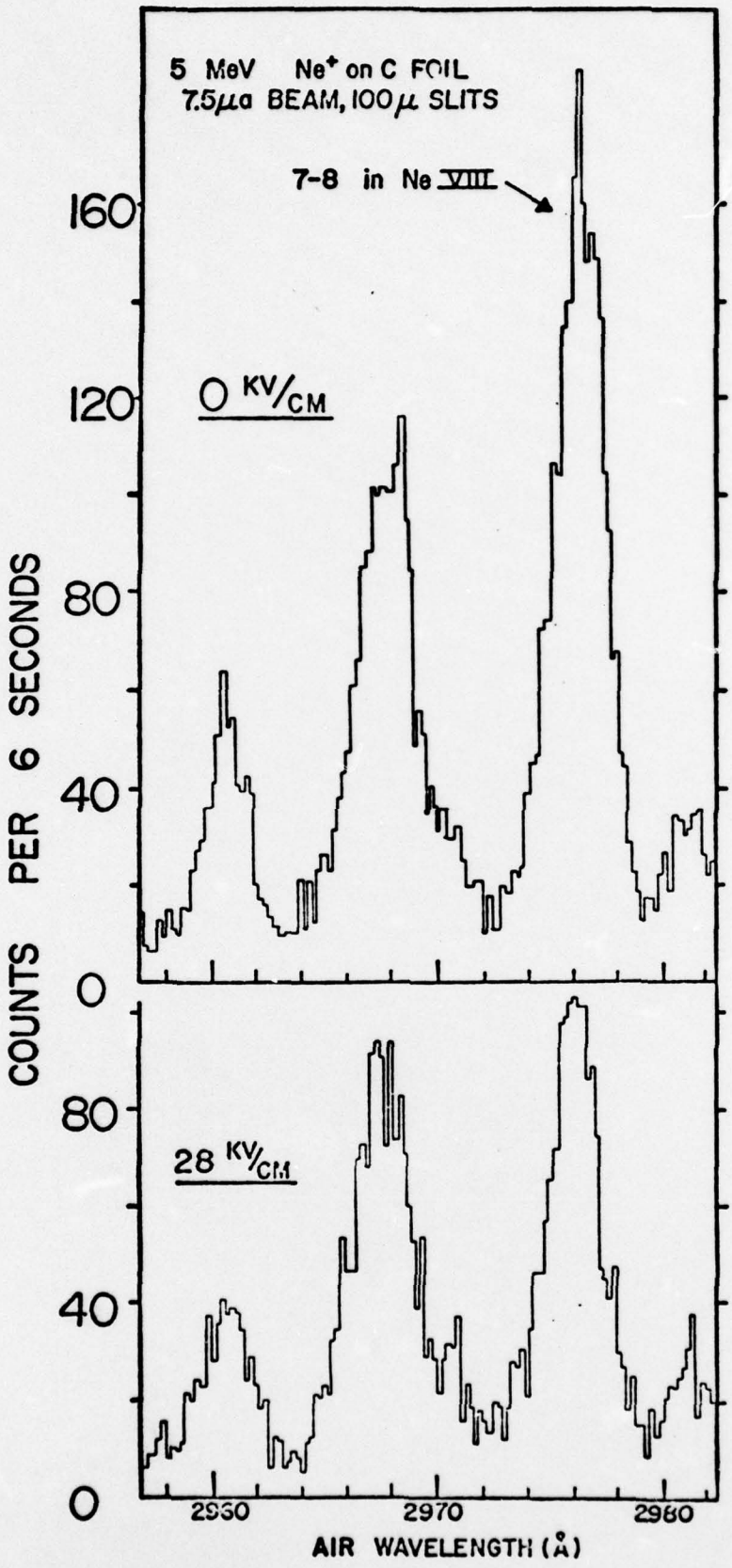
5 MeV Ne+ on C FOIL
7.5μa BEAM, 100μ SLITS
7-8 in Ne VIII
0 KV/CM
28 KV/CM
COUNTS PER 6 SECONDS
0
40
80
120
160
2960
2970
2980
AIR WAVELENGTH (Å)

Fig. 44

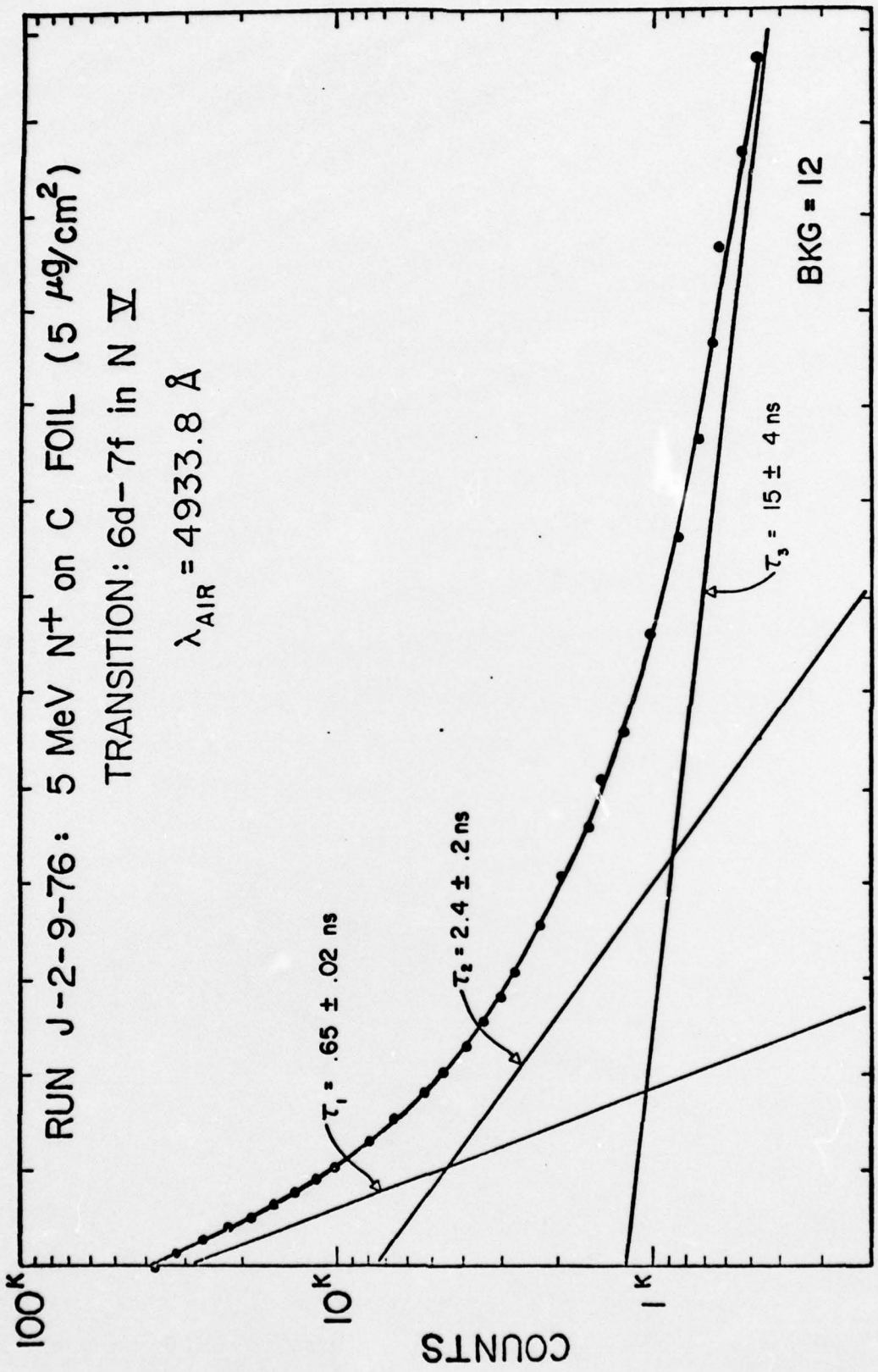
RUN J-2-9-76: 5 MeV N+ on C FOIL (5 μg/cm²)
TRANSITION: 6d-7f in N V
λAIR = 4933.8 Å
τ1 = .65 ± .02 ns
τ2 = 2.4 ± .2 ns
τ3 = 15 ± 4 ns
BKG = 12
100K
10K
1K
COUNTS
0
5
10
FOIL POSITION (CM)

Fig. 45

Summary of Measurements of Mean Lives of Levels in N V ($1s^2nl$)

n \ l →	s	p	d	f	g	h	i
10	1.84	1.46	.80	x 1.72	2.90	4.38	6.19
9	1.39	1.08	x .59	x 1.26	2.12	3.22	4.54
8	.98	x .77	x .41	x .89	1.50	2.27	3.21
7	x .68	xx .54	xxx .28	xxx .60	x 1.01	1.53	2.16
6	x .45	x .36	xx .18	xx .38	x .64	.97	
5	x .29	xx .22	x .10	x .22	x .38		
4	x .18	x .14	x .05	x .12			
3	.11	x .08	.02				
2	—	x 2.95					

Theoretical (Coulomb Approx)
Lifetimes in nanoseconds

Fig. 46

N V ($1s^2 nl$)

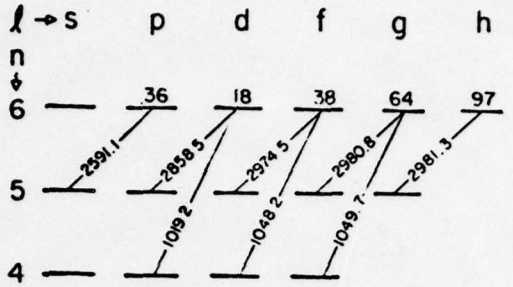

λ (Å)	Transition(s)	Experimental Mean Life(s) of Upper State (NS)	Theory (NS)
2991.1	5s – 6p	40 ± .02	36
2858.5	5p – 6d	.19 ± .01	18
2974.5	5d – 6f	.41 ± .02	38
2981	5fg – 6gh	.79 ± .04, .24 ± .4	64, .97
1048.2	4d – 6f	.46 ± .04	38
1049.7	4f – 6g	.72 ± .04	64
1049	4df – 6fg	.67 ± .04, .51 ± .5	.38, .64

Resolution (Å)	Wavelength Range (Å)
.5	400 – 2000
.5 – 1.5	2000 – 3000
1.5 – 2.0	3000 – 6000

Fig. 47

N V LIFETIMES — PRELIMINARY RESULTS

Transition	τ_1(ns)	τ_2(ns)	$I(0)$ (counts)	$\frac{BKG}{I(0)}$
2s-2p	(3.48 ± .05)	(24 ± .06)	30100	5×10^{-3}
3p-4s	.19 ± .02	6 ± 2	1835	5×10^{-4}
3s-4p	1.53 ± .015	7 ± 3	4920	2×10^{-4}
3p-4d	.059 ± .002	32 ± .03	48860	2×10^{-3}
3d-4f	1.1 ± .01	51 ± 10	2025	5×10^{-4}
4p-5s	(.31 ± .03)	(1.5 ± .4)	26500	6×10^{-4}
4s-5p	(.27 ± .01)	(1.2 ± .2)	36300	4×10^{-3}
4d-5p	(.28 ± .01)	(1.6 ± .3)	7010	5×10^{-3}
4p-5d	(.10 ± .01)	(.40 ± .15)	27300	4×10^{-3}
4f-5d	(.09 ± .03)	(.38 ± .09)	244	.05
4d-5f	.26 ± .01	1.3 ± .1	29860	3×10^{-4}
4f-5g	.43 ± .03	1.8 ± .3	33360	3×10^{-4}
5p-6s	.50 ± .01	2.5 ± .3	13300	7×10^{-3}
5s-6p	.40 ± .02	2.0 ± .5	840	.01
5p-6d	.20 ± .01	1.3 ± .3	5430	2×10^{-3}

Transition	τ_1(ns)	τ_2(ns)	$I(0)$ (counts)	$\frac{BKG}{I(0)}$
5d-6f	.41 ± .02	1.6±0.2	55 520	2×10^{-3}
4d-6f	.48 ± .05	4 ±2	658	.03
4d-6g	.71 ± .06	4 ±2	862	.03
6g-7h	.74 ± .03	—	625	.04
6s-7p	.61 ± .02	1.9 ±.4	3[illegible]37	3×10^{-3}
6d-7p	.61 ± .03	6 ±2	7[illegible]40	.01
6p-7d	.52 ± .02	2.5± .7	[illegible]715	.01
6f-7g	.27 ± .04	4.0±0.5	1[illegible]40	.01
5p-7s	.30 ± .02	2.0±0.3	2[illegible]70	7×10^{-4}
6d-7f	.44 ± .02	2.2±.2	9[illegible]05	4×10^{-4}
5d-7f	1.62 ± .04)	(2.1±0.3)	13 [illegible]40	8×10^{-3}
6s-8p	.78 ± .04	9 ±3	2[illegible]90	.03
6p-8d	.48 ± .05	1.9±0.6	8[illegible]40	.01
6s-8f	1.06 ± .03	7.1±0.5	7[illegible]40	.03
7s-9f	1.15 ± .15	46 ±6	1[illegible]50	.3
6d-10f	2.2 ± .4	8 ±3	560	.01

Fig. 48

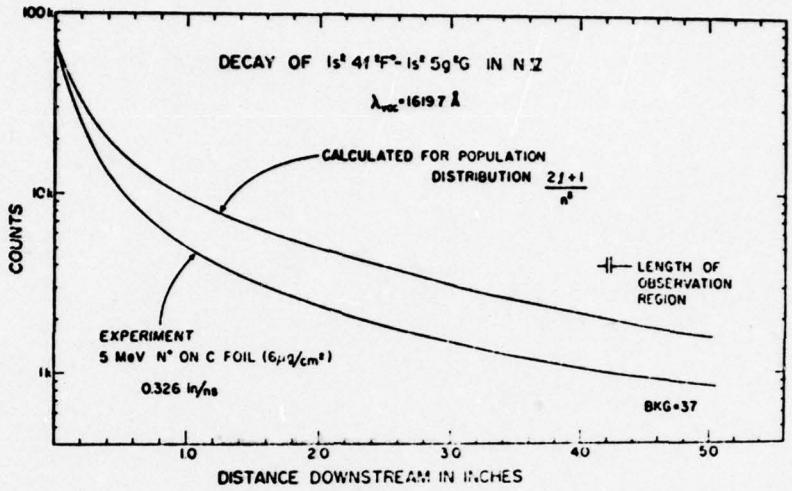
DECAY OF $1s^2 4f\,^2F^o - 1s^2 5g\,^2G$ IN N I
λ_{vac} = 16197 Å
CALCULATED FOR POPULATION DISTRIBUTION $\frac{2J+1}{n^3}$
LENGTH OF OBSERVATION REGION
EXPERIMENT
5 MeV N° ON C FOIL (6μg/cm²)
0.326 in/ns
BKG=37
COUNTS
100k
10k
1k
10
20
30
40
50
DISTANCE DOWNSTREAM IN INCHES

Fig. 49

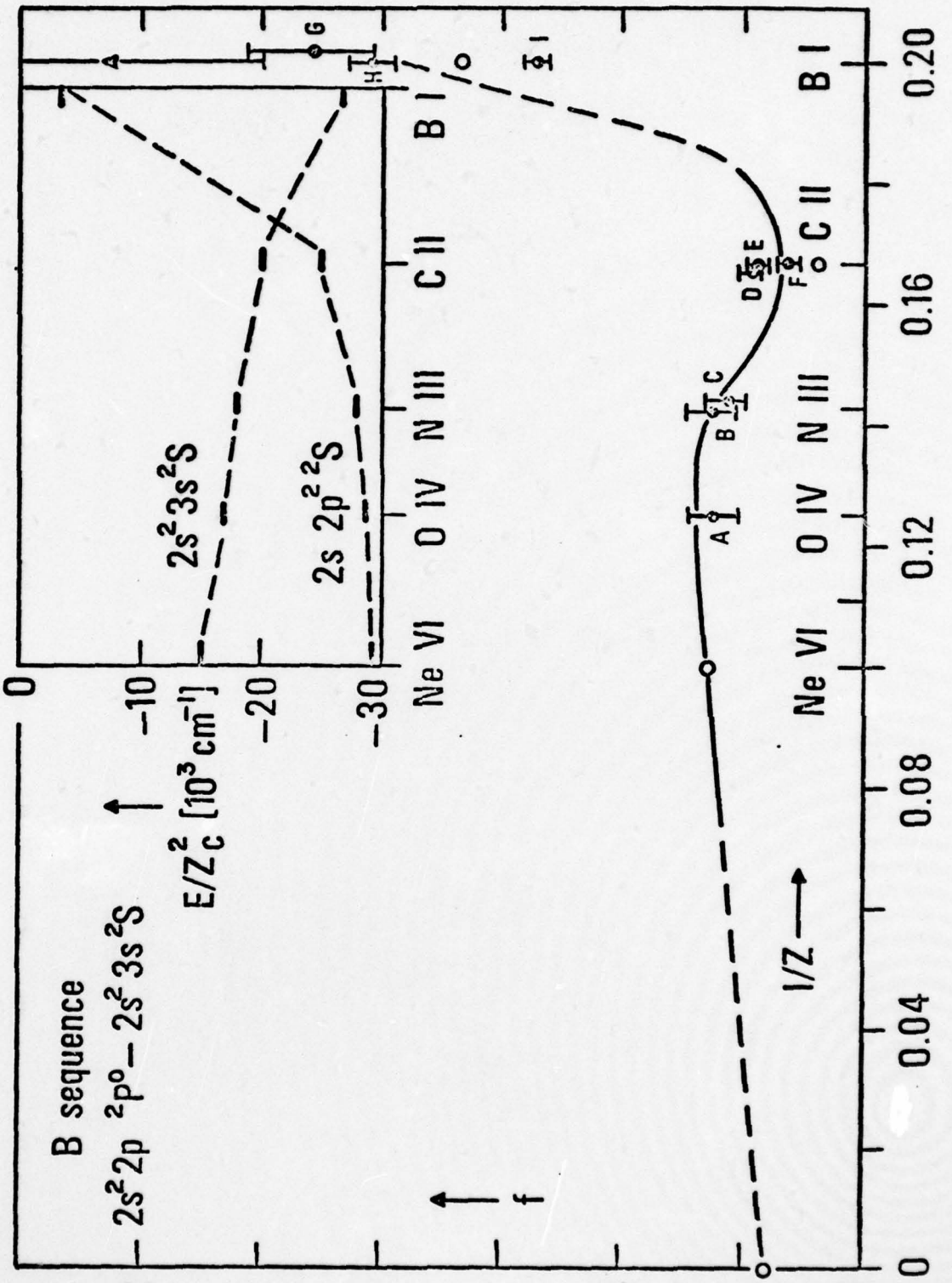
B sequence
$2s^2 2p\ ^2p^o - 2s^2 3s\ ^2S$
E/Z_c^2 [10^3 cm^{-1}]
$2s^2 3s\ ^2S$
$2s\ 2p^2\ ^2S$
Ne VI
O IV
N III
C II
B I
f
I/Z
A
B
C
D
E
F
G
H

Fig. 50

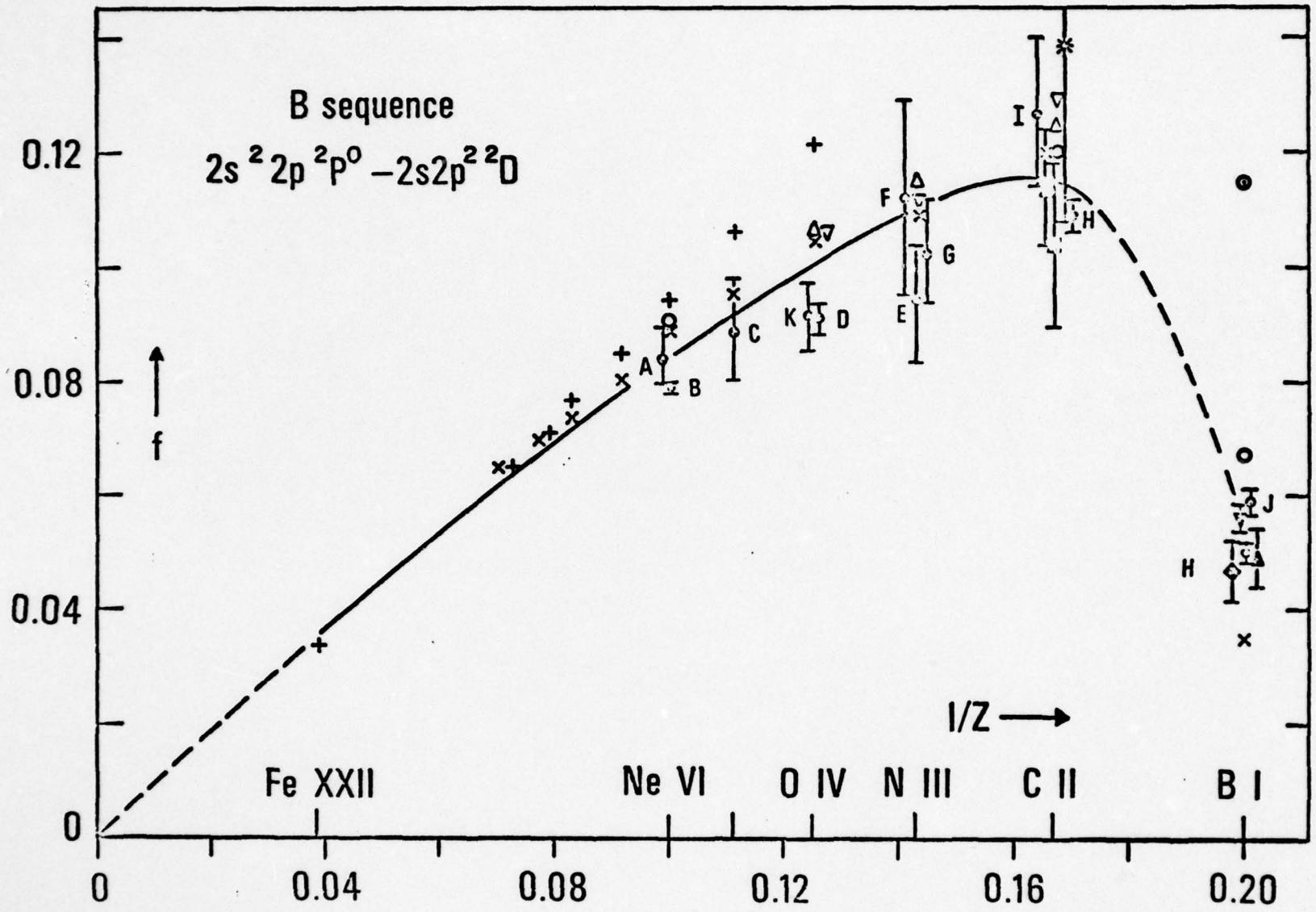
B sequence
2s ² 2p ²P° – 2s2p² ²D
0.12
0.08
0.04
0
f
I/Z →
Fe XXII
Ne VI
O IV
N III
C II
B I
0
0.04
0.08
0.12
0.16
0.20
A
B
C
D
E
F
G
H
I
J
K

Fig. 51

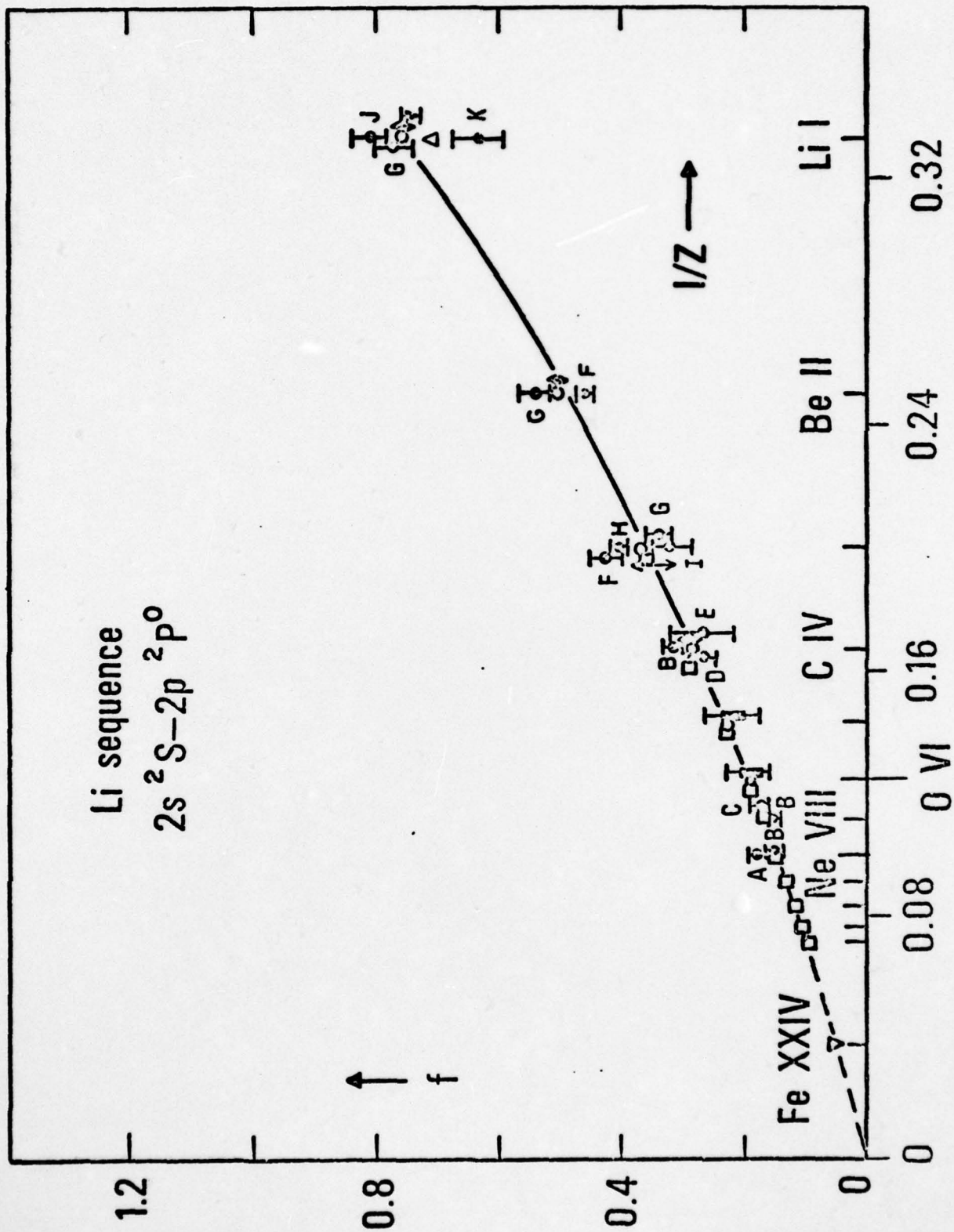
Li sequence
2s ²S–2p ²P°
f
1.2
0.8
0.4
0
Fe XXIV
Ne VIII
O VI
C IV
Be II
Li I
0
0.08
0.16
0.24
0.32
I/Z

Fig. 52

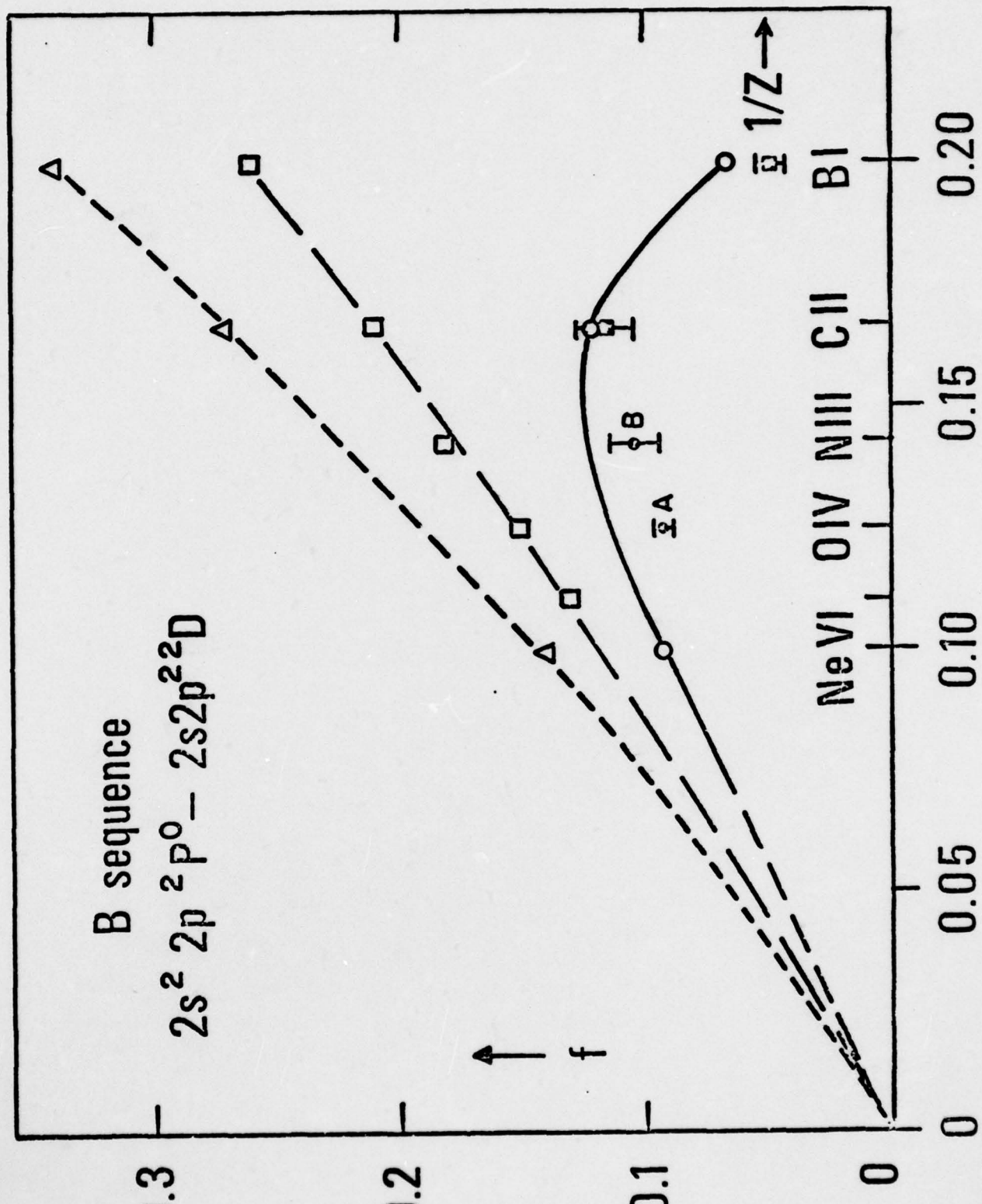
B sequence
$2s^2\ 2p\ ^2P^o - 2s2p^2\ ^2D$
f
0.3
0.2
0.1
0
0
0.05
0.10
0.15
0.20
Ξ 1/Z
NeVI OIV NIII CII BI
Ξ_A
Ξ_B

Fig. 53

REFERENCES

1. I. Sellin, Topics in Current Physics, I: Beam-Foil Spectroscopy, Ed. S. Bashkin, Springer Verlag (Heidelberg, 1976), Chapt. 10.
2. S. Bashkin, D. Fink, P. R. Malmberg, A. B. Meinel, and S. G. Tilford, J. Opt. Soc. Am. 56, 1064 (1966).
3. J. O. Stoner, Jr. and J. A. Leavitt, Appl. Phys. Letters 18, 447 (1971).
4. J. A. Leavitt, J. W. Robson, and J. O. Stoner, Jr., Nucl. Instr. Methods 110, 423 (1973).
5. J. O. Stoner, Jr. and J. A. Leavitt, Optica Acta 20, 435 (1973).
6. J. O. Stoner, Jr. and J. A. Leavitt, Appl. Phys. Letters 18, 360 (1971).
7. P. R. Malmberg, S. Bashkin, and S. G. Tilford, Phys. Rev. Letters 15, 98 (1965).
8. J. A. Leavitt and B. S. Cardon, private communication.
9. S. Bashkin, G. W. Carriveau, and H. J. Hay, J. Phys. B 4, L32 (1971).
10. S. Bashkin and J. A. Leavitt, unpublished.
11. S. Bashkin and G. Beauchemin, Can. J. Phys. 44, 1603 (1966).
12. W. S. Bickel and S. Bashkin, Phys. Rev. 162, 12 (1967).
13. B. Engman, A. Gaupp, L. J. Curtis, and I. Martinson, to be published.
14. R. Buchta, I. Martinson, and S. Bashkin, unpublished.
15. I. Martinson, Topics in Current Physics, I: Beam-Foil Spectroscopy, Ed. S. Bashkin, Springer Verlag (Heidelberg, 1976), Chapt. 2.

16. L. J. Curtis, I. Martinson, and R. Buchta, Nucl. Instr. Methods 110, 391 (1973).

17. T. Andersen and G. Sørenson, Solar Physics 38, 343 (1974).

18. T. Andersen, O. Poulsen, P. S. Ramanujam, and A. Petkov Petrakiev, Solar Phys. 44, 257 (1975).

19. B. Engman, J. O. Stoner, Jr., and I. Martinson, Physica Scripta 13, 363 (1976).

20. T. Andersen, Nucl. Instr. Methods 110, 35 (1973), and references therein.

21. B. L. Cardon and J. A. Leavitt, Bull. Opt. Soc. of America, p. 1067 (1976).

22. L. C. McIntyre and E. M. Bernstein, private communication.

23. P. M. Griffin, D. J. Pegg, I. A. Sellin, K. W. Jones, D. J. Pisano, T. H. Kruse, and S. Bashkin, Beam-Foil Spectroscopy, Vol. 1, Eds. I. A. Sellin and D. J. Pegg, Plenum Press (New York, 1975), p. 321.

24. S. Bashkin, K. W. Jones, T. H. Kruse, J. A. Leavitt, and D. J. Pisano, to be published.

25. Such an experiment has now been done by K. W. Jones and collaborators. Private communication.

26. S. Bashkin, K. W. Jones, T. H. Kruse, D. J. Pegg, D. J. Pisano, and I. A. Sellin, to be published.

27. S. Bashkin, J. Bromander, J. A. Leavitt, and I. Martinson, Physica Scripta 8, 285 (1973).

28. S. Bashkin, W. S. Bickel, and B. Curnutte, J. Opt. Soc. Am. 59, 879 (1969).

29. H. G. Berry, J. Opt. Soc. Am. 61, 983 (1971).

30. B. I. Dynefors and I. Martinson, to be published.

31. W. S. Bickel, S. Bergström, R. Buchta, L. Lundin, and I. Martinson, Phys. Rev. 178, 118 (1969).

32. H. G. Berry, I. Martinson, L. J. Curtis, and L. Lundin, Phys. Rev. A 3, 1934 (1971).

33. E. J. Knystautas and R. Drouin, Nucl. Instr. Methods 110, 95 (1973).

34. H. G. Berry, J. Desesquelles, and M. Dufay, Phys. Rev. A 6, 600 (1972).

35. I. Martinson, Physica Scripta 9, 281 (1974).

36. S. Bashkin, L. Heroux, and J. Shaw, Phys. Letters 13, 229 (1964).

36A. M. Druetta, M. C. Poulizac, and P. Ceyzeriat, J. Phys. B. 4, 1070 (1971).

37. B. Emmoth, M. Braun, J. Bromander, and I. Martinson, Physica Scripta 12, 75 (1975).

38. T. Andersen, A. Petrakiev Petkov, and G. Sørensen, Physica Scripta 12, 284 (1975).

39. J. R. Roberts, T. Andersen, and G. Sørensen, Nucl. Instr. Methods 110, 119 (1973).

40. M. Dufay, A. Denis, and J. Desesquelles, Nucl. Instr. Methods 90, 85 (1970).

41. H. G. Berry, R. M. Schectman, I. Martinson, W. S. Bickel, and S. Bashkin, J. Opt. Soc. Am. 60, 335 (1970).

42. I. Martinson, private communication.

43. S. Bashkin, Beam-Foil Spectroscopy, Vol. 1, Eds. J. A. Sellin and D. J. Pegg, Plenum Press (New York, 1975), p. 129.

44. J. A. Leavitt, private communication.

45. J. A. Leavitt and D. Dietrich, private communication.

46. W. Wiese, Topics in Current Physics, I: Beam-Foil Spectroscopy, Ed. S. Bashkin, Springer Verlag (Heidelberg, 1976), Chapt. 5.

47. R. Marrus, Topics in Current Physics, I: Beam-Foil Spectroscopy, Ed. S. Bashkin, Springer Verlag (Heidelberg, 1976), Chapt. 8.

48. W. Whaling, R. B. King, and M. Martinez-Garcia, Astrophys. J. 158, 389 (1969).